Sensor and Simulation Notes

Note 159

October 1972

Pulse Radiation By An Infinite Cylindrical Antenna With A Source Gap with a Uniform Field

Zoe Lynda Pine
Fred M. Tesche

The Dikewood Corporation

Abstract

The radiated electric field is calculated for an infinite cylindrical antenna driven by a step-function voltage applied across a finite gap. Plots of the time history of the radiated field for various gap sizes and observation angles are presented, and both the early and late time asymptotic fields are investigated.

I. Introduction

Much effort has been expended previously to predict the radiation field for a cylindrical antenna designed to simulate the electromagnetic pulse due to a nuclear explosion.[1,2] Results have been obtained for the infinite cylindrical antenna driven by a step-function voltage applied across an infinitesimal gap. In this note, an attempt is made to develop a closer approximation to the real antenna by assuming a finite gap infinite antenna. The gap is excited by an electric field which is a step-function of time and is uniform over the gap.

In Section II, an analysis of the problem is given with a detailed study of the antenna described above. Section III is concerned with the numerical techniques used in calculating the results described in Section V. In addition, an alternate method for treating this problem is described in Section IV.

II. Theoretical Analysis

This section is concerned with the transient radiation field of an infinite antenna excited by a step-function over a finite source gap. We begin with the equation for the radiation field of a similar antenna excited by a step-function electric field of magnitude E_o over an infinitesimal gap of width δ, which is given by Ref. (1) as

$$rE_\theta = \frac{E_o \delta}{2\sin\theta} \int_o^\infty \frac{e^{-\xi q \csc \theta} I_o(\xi)}{K_o^2(\xi) + \pi^2 I_o^2(\xi)} \frac{d\xi}{\xi} U(q + \sin\theta) . \qquad (1)$$

Note that in this equation, $q = (ct - r)/a$ where a is the radius of the antenna and r is the distance from the antenna to the observer. θ is the angle of observation and I_o and K_o are modified Bessel functions. This note considers only the radiated fields at the far field observer. Figure 1 shows the geometry of the problem under consideration.

Assuming that in the finite gap region there are an infinite number of infinitesimal gaps, the radiation field generated by the entire finite gap can be obtained by integrating the results of the delta gap over the finite source region. From Figure 1, it is seen that the following can be assumed:

1. $\theta \approx \theta_o$
2. $r \sim r_o$ except for the r in the exponential
3. $r = \sqrt{r_o^2 + z^2 - 2r_o z \cos\theta} \approx r_o - z\cos\theta$ for the exponential r.
4. $E_o \longrightarrow V_o/\Delta$ (for assumed uniform field distribution)
5. $\delta \longrightarrow dz$.

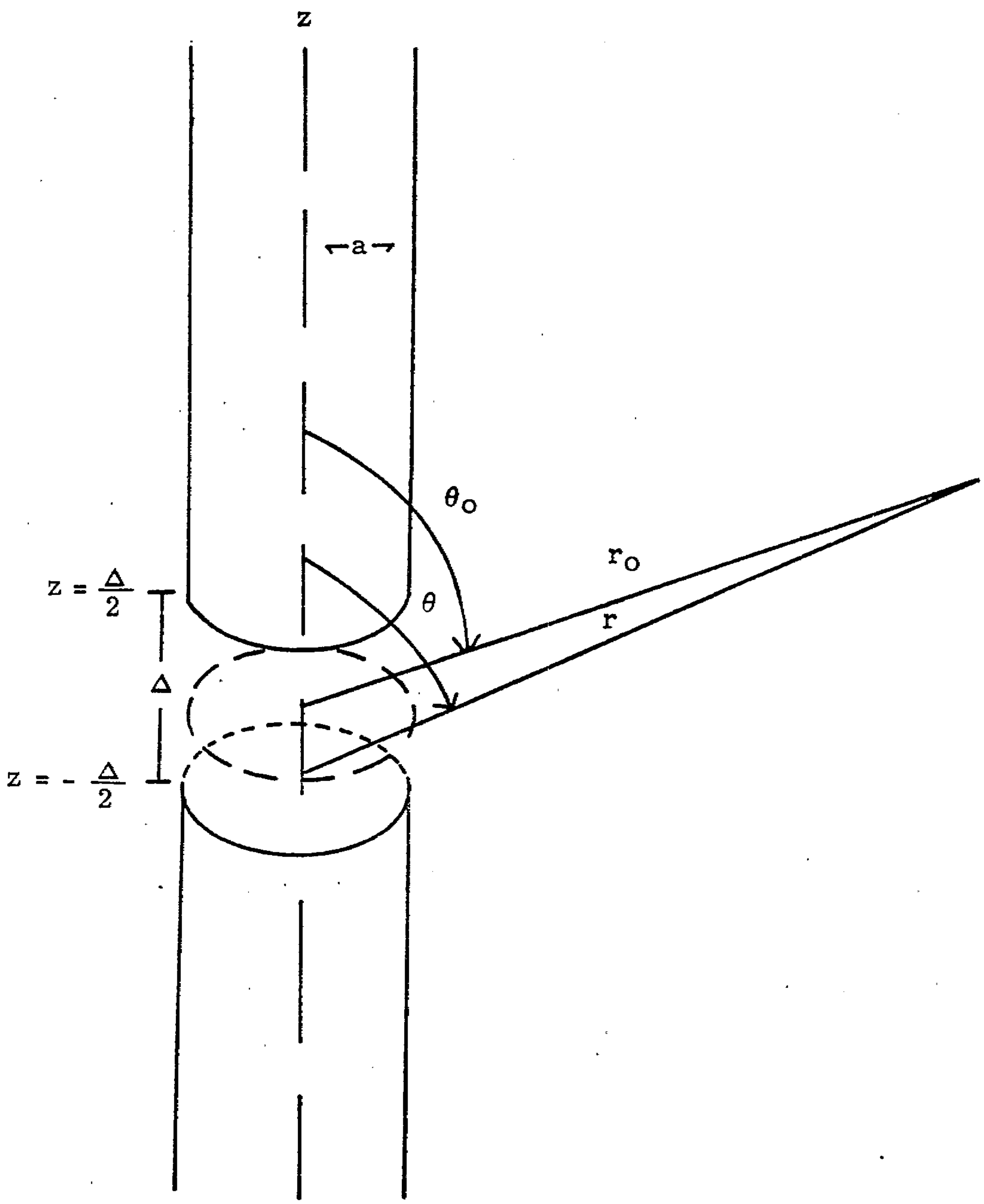

Figure 1. Infinite Antenna With a Finite Gap

Integrating Equation (1) over the gap with the above assumptions gives

$$\frac{rE_\theta}{V_o} = \frac{1}{2\Delta \sin\theta} \int_{-\Delta/2}^{\Delta/2} dz \int_0^\infty \frac{e^{-\xi\left(\frac{ct - r_o + z\cos\theta}{a}\right)\csc\theta} I_o(\xi)}{K_o^2(\xi) + \pi^2 I_o 2(\xi)} \frac{d\xi}{\xi} \cdot U\left(\frac{ct - r_o + z\cos\theta}{a} + \sin\theta\right) \quad (2)$$

Equation (2) can be simplified by defining $\tau = \frac{ct - r_o}{a}$, and $p = (\tau + \frac{z\cos\theta}{a})$ $\csc\theta$. Equation (2) then becomes

$$\frac{rE_\theta}{V_o} = \frac{1}{2\Delta\sin\theta} \int_{\Delta/2}^{\Delta/2} dz \int_0^\infty \frac{e^{-\xi p} I_o(\xi)}{K_o^2(\xi) + \pi^2 I_o 2(\xi)} \frac{d\xi}{\xi} \, U(p\sin\theta + \sin\theta) \quad (3)$$

Let $F(p) = \int_0^\infty \frac{e^{-\xi p} I_o(\xi)}{K_o^2(\xi) + \pi^2 I_o^2(\xi)} \frac{d\xi}{\xi}$, and substituting in

equation (3) gives

$$\frac{rE_\theta}{V_o} = \frac{1}{2\Delta/\sin\theta} \int_{-\Delta/2}^{\Delta/2} dz \quad F(p) \; U(p\sin\theta + \sin\theta). \quad (4)$$

This equation defines the far field radiation from the infinite antenna with a source gap of finite width, Δ, and a uniform field distribution.

Behavior of rE/V_o for $\theta = \pi/2$:

When $\theta = \pi/2$, the far field observer sees the contributions from all of the infinitesimal gaps simultaneously, which leads to the conclusion that for $\theta = \pi/2$, the result for the finite gap is similar to that for the infinitesimal gap. That is, the radiated field is infinite in magnitude at the first instant the observer sees it and it then diminishes as time goes on.

To see this effect, let $\theta \to \pi/2$. Then $U(p \sin\theta + \sin\theta) \to U(\tau + \sin\theta)$. By assumption (2), $U(\tau + \sin\theta) \approx U(q + \sin\theta)$. Also, $F(p) = F\left(\tau + \frac{z\cos\theta}{a}\right) \to F(\tau) = F\left(\frac{ct - r_o}{a}\right)$. Equation (4) becomes

$$\lim_{\theta \to \pi/2} \frac{rE_\theta}{V_o} = \frac{F(\tau)}{2\Delta \sin\theta} \int_{-\Delta/2}^{\Delta/2} dz \;\; U(q + \sin\theta) = \frac{1}{2\sin\theta} \;\; F(\tau)\, U(q + \sin\theta). \tag{5}$$

Also note that $F\left(\frac{ct - r_o}{a}\right) = F\left(\frac{ct - r + z\cos\theta}{a}\right) \to F\left(\frac{ct - r}{a}\right) = F(q)$ as $\theta \to \pi/2$. Thus, as expected,

$$\lim_{\theta \to \pi/2} \frac{rE_\theta}{V_o} = \frac{1}{2} \qquad F(q)\, U(q + 1). \tag{6}$$

Since the equation for $\theta = \pi/2$ in the finite gap case the same as in the infinitesimal gap, it can be concluded that the early and late time asymptotic forms are also identical to those of the infinitesimal gap.

Early Time Behavior of rE/V_o:

Since the integration of equation (1) is over a finite gap region, the early time behavior of that equation must be considered. The asymptotic early time form of equation (1) is given as[1]

$$rE_\theta = \frac{E_o \delta}{2\sin\theta} \;\; \frac{\sqrt{2}}{\pi} \;\; \frac{1}{\sqrt{q \csc\theta + 1}} \;\; U(q + \sin\theta). \tag{7}$$

Using the earlier assumptions, and integrating over the finite source region, this becomes

$$\frac{rE_\theta}{V_o} = \frac{1}{2\sin\theta}\ \frac{\sqrt{2}}{\pi} \int_{-\Delta/2}^{\Delta/2} \frac{1}{\sqrt{p+1}}\ dz\ U\ (p \sin\theta + \sin\theta\ ). \qquad (8)$$

It is obvious from equation (8), that a discontinuity exists at $p = -1$. If one thinks of the integration as a window which moves along the p-axis, as shown in Figure 2, one clearly sees the discontinuity when $p = -1$ is in the center of the window. As will be discussed more fully in Section III, for $p < -1$, the step-function is not "turned on". So when the window straddles $p = -1$, the only section considered is $-1 \leq p \leq p_1$. The discontinuity in this section can be handled by subtracting the asymptotic form, equation (8) from F(p). Equation (4) becomes

$$\frac{rE_\theta}{V_o} = \frac{1}{2\Delta\sin\theta}\left[\int_{-\Delta/2}^{\Delta/2}\left(F(p) - \frac{\sqrt{2}}{\pi}\ \frac{1}{\sqrt{p+1}}\right) dz\ \ U(p \sin\theta + \sin\theta) \right.$$
$$\left. + \frac{\sqrt{2}}{\pi}\int_{-\Delta/2}^{\Delta/2} \frac{1}{\sqrt{p+1}}\ dz\ \ U(p \sin\theta + \sin\theta)\right] \qquad (9)$$

Equation (9) determines the radiated field for the antenna under consideration. Using this form, one avoids the numerical trouble arising from the discontinuity at $p = -1$.

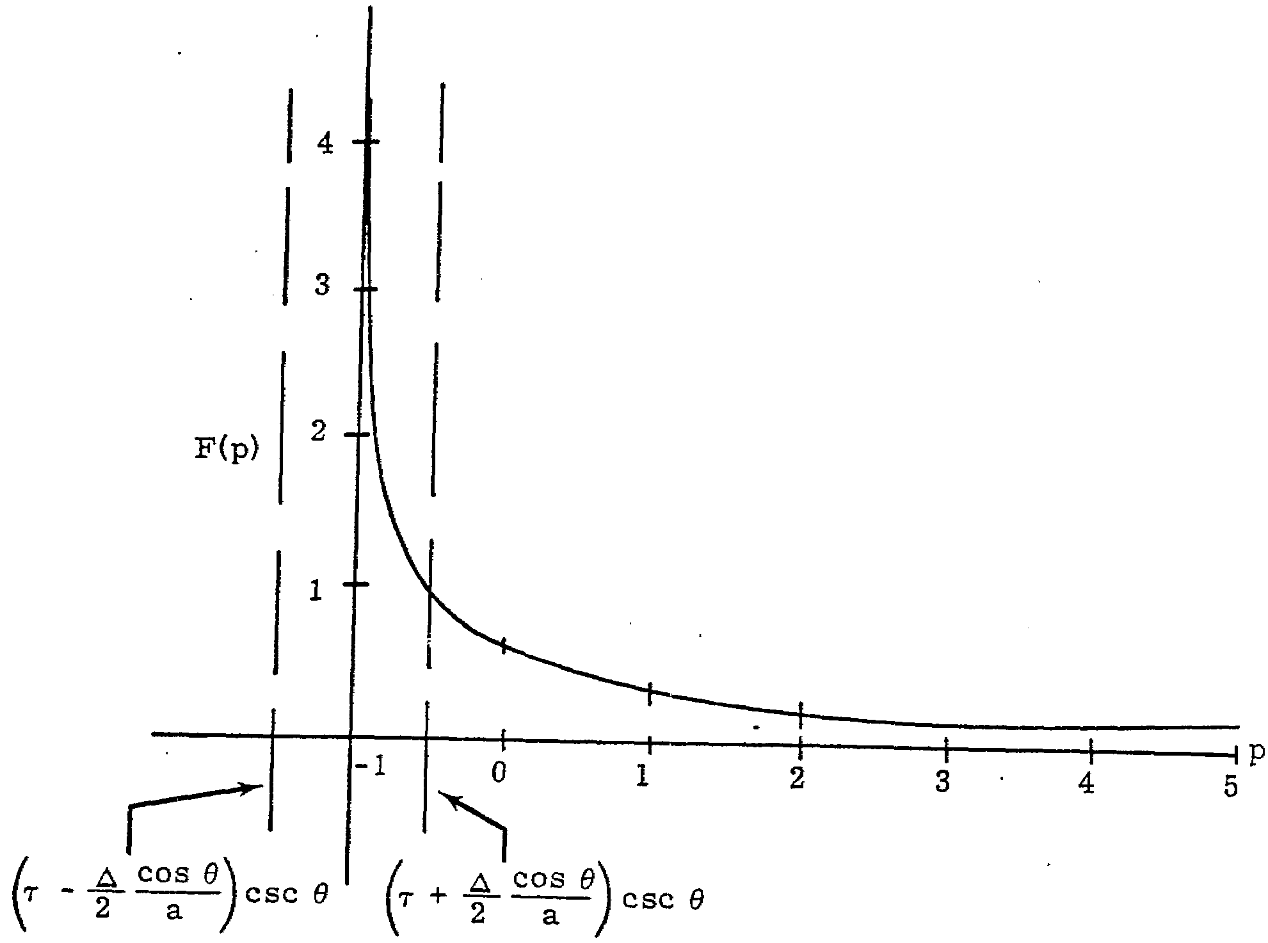

Figure 2. Imaginary Window Scanning F(p)

Late Time Behavior:

The late time asymptotic form for the infinitesimal gap is given by[1]

$$rE_\theta = \frac{E_o \delta}{2\sin\theta} \quad \frac{1}{\ell n\left(\frac{2(q+1)}{\Gamma \sin\theta}\right)} \; . \tag{10}$$

Using the assumptions given earlier, the form for the finite gap is given by

$$\frac{rE_\theta}{V_o} = \frac{1}{2\Delta\sin\theta} \int_{-\Delta/2}^{\Delta/2} \frac{1}{\ell n\left(\frac{2\left(\frac{ct-r_o}{a}+1\right)}{\Gamma\sin\theta}\right)} dz \cdot U\left(\frac{ct-r_o}{a} + \sin\theta\right). \tag{11}$$

But $\frac{ct-r_o}{a} = \tau$ and equation (11) becomes

$$\frac{rE_\theta}{V_o} = \frac{1}{2\,\Delta\sin\theta} \int_{-\Delta/2}^{\Delta/2} \frac{1}{\ell n\left(\frac{2(\tau+1)}{\Gamma\sin\theta}\right)} dz \;\; U\left(\frac{ct - r_o + z\cos\theta}{a} + \sin\theta\right) \tag{12}$$

which reduces to

$$\frac{rE_\theta}{V_o} = \frac{1}{2\sin\theta} \quad \frac{1}{\ell n\left(\frac{2(\tau+1)}{\Gamma\sin\theta}\right)} \quad U\left(\frac{ct - r_o + z\cos\theta}{a} + \sin\theta\right). \tag{13}$$

III. Numerical Techniques

A time-saving technique was used in the evaluation of $F(p) - \frac{\sqrt{2}}{\pi} \frac{1}{\sqrt{p+1}}$. A table was set up such that $f(p) = F(p) - \frac{\sqrt{2}}{\pi} \frac{1}{\sqrt{p+1}}$. f(p) was calculated at evenly spaced values of p denoted by p_n with $p_1 = -1 + \epsilon$. Since f(p) is a smooth function, a linear interpolation was used to arrive at a point x, where $p_n < x < p_n + 1$. Thus the function F(p) need not be calculated for every set of gap sizes and angles.

In calculating F(p), the code developed for $F(\xi)$, which in this note will be called $G(\xi)$, in Sensor and Simulation Note 110 was used with a slight change. Where the $G(\xi)$ code was used to calculate

$$G(\xi) = \int_0^\infty \frac{e^{-y(\xi - 1)} I_o(y)}{\pi^2 I_o^2(y) + K_o^2(y)} \frac{dy}{y}, \tag{14}$$

the expression

$$F(p) = \int_0^\infty \frac{e^{-y(p)} I_o(y)}{\pi^2 I_o^2(y) + K_o^2(y)} \frac{dy}{y} \tag{15}$$

was needed. So a slight change was effected where $\xi = p + 1$ and thus the code evaluates

$$F(p) = G(\xi) = \int_0^\infty \frac{e^{-y(\xi-1)} I_o(y)}{\pi^2 I_o(y) + K_o^2(y)} \frac{dy}{y} \tag{16}$$

By substituting f(p) into equation (9), this becomes

$$\frac{rE_\theta}{V_o} = \frac{1}{2\Delta\sin\theta} \left[\int_{-\Delta/2}^{\Delta/2} f(p)\, dz\, U(p \sin\theta + \sin\theta) \right.$$

$$\left. + \frac{\sqrt{2}}{\pi} \int_{-\Delta/2}^{\Delta/2} \frac{1}{\sqrt{p+1}}\, dz\, U(p \sin\theta + \sin\theta) \right] \tag{17}$$

With

$$dz = \frac{a \sin\theta}{\cos\theta} \, dp$$

$$P1 = (\tau + \frac{\Delta}{2a} \cos\theta) \csc\theta$$

$$P2 = (\tau - \frac{\Delta}{2a} \cos\theta) \csc\theta$$

equation (7) becomes

$$\frac{rE_\theta}{V_o} = \frac{a}{2\Delta\cos\theta}\left[\int_{P2}^{P1} f(p)\, dp\, U(p \sin\theta + \sin\theta)\right.$$

$$\left. + \frac{\sqrt{2}}{\pi}\int_{P2}^{P1} \frac{1}{\sqrt{p+1}}\, dp\, U(p\sin\theta + \sin\theta)\right] \tag{18}$$

It can easily be seen at this point that the field is symmetric around $\theta = 90°$. For $90° < \theta < 180°$ it is noted that

$$\begin{aligned} P1 &= (\tau + \frac{\Delta}{2a} \cos\theta) \csc\theta = (\tau - \frac{\Delta}{2a} |\cos\theta|) \csc\theta \\ P2 &= (\tau - \frac{\Delta}{2a} \cos\theta) \csc\theta = (\tau + \frac{\Delta}{2a} |\cos\theta|) \csc\theta \end{aligned} \tag{19}$$

This causes the value of the integral to be negative. But the constant, $\frac{\Delta}{2a} \cos\theta$, is negative and so the result is the same for $90° + x$ as for $90° - x$. However, a treatment of the step-function must include the ability to handle P1 and P2 properly. In other words, the code must integrate from the lesser to the greater and not blindly from P2 or P1.

At this point, a more detailed discussion of the step-function should be given for $0° < \theta < 90°$. It is noted that $p \sin\theta + \sin\theta = 0$ implies that $p = -1$. By defining a variable, P3, as the maximum of P2 and -1, ($P3 = \max\{P3, -1\}$), equation (18) is simplified as follows.

$$\frac{rE_\theta}{V_o} = 0 \qquad \text{for } P1 < -1$$

$$\frac{rE_\theta}{V_o} = \frac{a}{2\Delta\cos\theta}\left[\int_{P3}^{P1} f(p)\, dp + \frac{\sqrt{2}}{\pi}\int_{P3}^{P1} \frac{1}{\sqrt{p+1}}\, dp\right]. \tag{20}$$

It is important to note that for P3 or P1 equal -1 a close-ended quadrature would result in a discontinuity. Therefore, an open-ended quadrature should be used.

Now, let $I = \displaystyle\int_{P3}^{P1} \frac{1}{\sqrt{p+1}}\, dp$ and calculate I analytically. The result is

$$I = 2\left(\sqrt{P1+1} - \sqrt{P3+1}\right). \tag{21}$$

Using this, equation (18) can be further simplified as

$$\frac{rE_\theta}{V_o} = \frac{a}{2\Delta\cos\theta}\left[\int_{P3}^{P1} f(p)\, dp + \frac{2\sqrt{2}}{\pi}\left(\sqrt{P1+1} - \sqrt{P3+1}\right)\right]. \tag{22}$$

The results given in this note were obtained by programming equation (22). The window technique was used to scan along the F(p) curve between the limits of integration within the turned on step-function. This technique combined with the treatment of the singularity and an open-ended quadrature will generate no numerical difficulties and will result in a fast running code. The total CP time on the CDC 6600 at Kirtland AFB was approximately 2 minutes for 28 combinations of gap size and angles.

IV. An Alternate Approach

Instead of obtaining the solution to the problem in question by integrating the function F(p) over the finite source gap, it has been pointed out by Baum that the response for any gap size can be obtained from the response of an antenna with a semi-infinite gap as shown in Figure 3. The equation for the radiated field from this equation is given by

$$\frac{rE_\theta}{E_{tan}} = \frac{1}{2 \sin\theta} \int_{-\infty}^{z} dz \int_{0}^{\infty} \frac{e^{-\xi p} I_o(\xi)}{K_o^2(\xi) + \pi^2 I_o^2(\xi)} \frac{d\xi}{\xi} \, U(p \sin\theta + \sin\theta) \quad (23)$$

where E_{tan} is the tangential electric field specified on the surface of the semi-infinite gap. Using the change in variables described in Section II, this becomes

$$\frac{rE_\theta}{E_{tan}} = \frac{1}{2 \sin\theta} \int_{-\infty}^{P1} F(p)\, dp \, U(p \sin\theta + \sin\theta) \quad (24)$$

where $P1 = \left(\tau + \frac{z \cos\theta}{a}\right) \cdot \csc$

Thus

$$\frac{rE_\theta}{E_{tan}} = 0 \quad \text{when } \tau \le -1$$

and (25)

$$\frac{rE_\theta}{E_{tan}} = \frac{1}{2 \sin\theta} \int_{-\infty}^{P1} F(p)\, dp \qquad \text{when } \tau > -1.$$

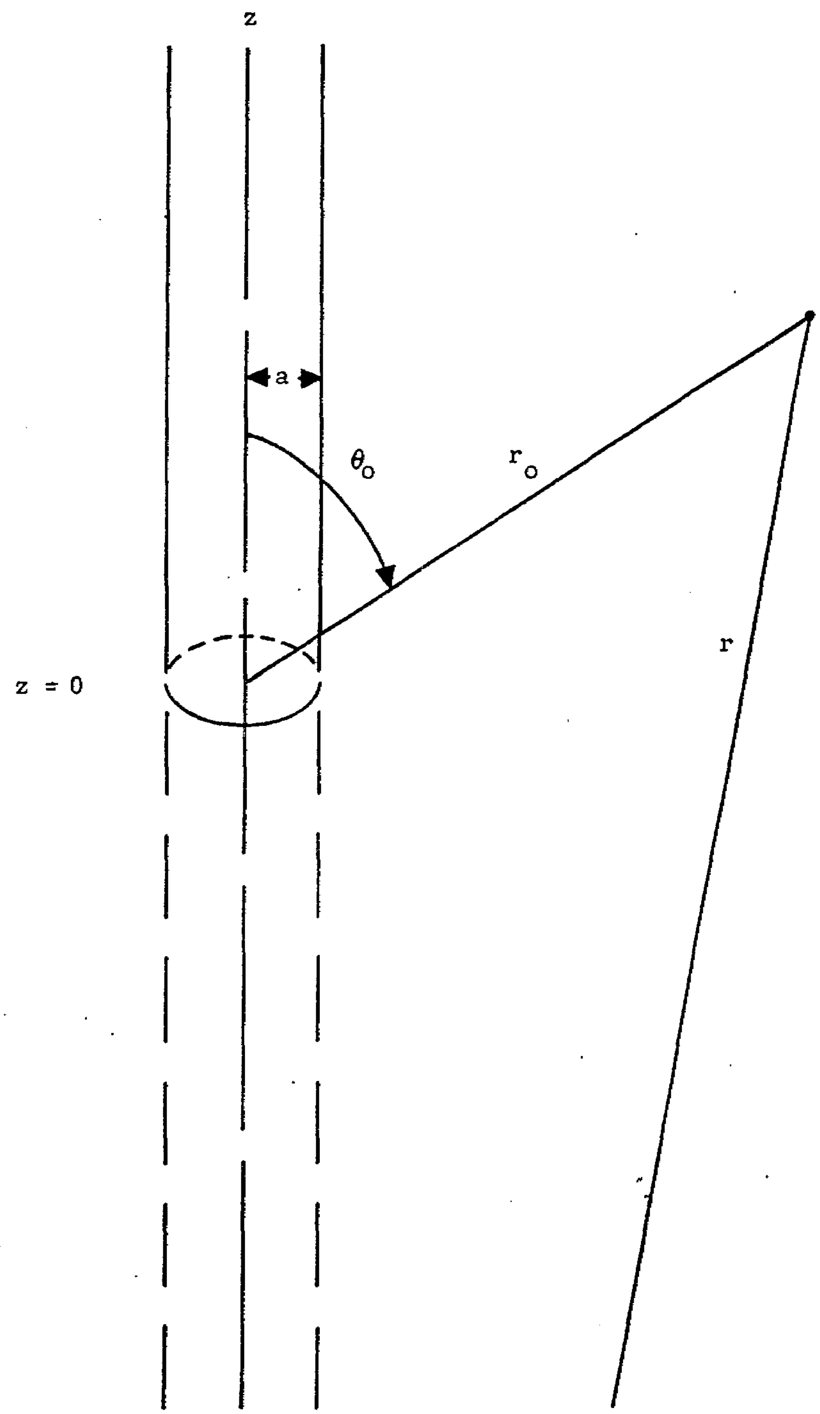

Figure 3. Infinite Antenna with Semi-Infinite Gap

Using equation 25, one can set up a table of $\frac{rE_\theta}{E_{tan}}$ for specific θ's and time. This was done for several angles and the results are shown in graphic form in Figures 24 to 26.

Assuming the table has been created, the results for a finite gap can be obtained by two simple time shifts and a subtraction. Let TS (θ, t) be the function represented in the table. For a finite gap, Δ , the result is given by

$$\frac{rE_\theta}{E_{tan}} = TS\,(\theta,\ t + \Delta/2 \cos\theta) - TS\,(\theta,\ t - \Delta/2 \cos\theta). \tag{26}$$

Note that for a finite gap $E_{tan} = V_o/\Delta$ and equation (26) becomes

$$\frac{rE_\theta}{V_o} = \frac{1}{\Delta}\left(TS\,(\theta,\ t + \Delta/2 \cos\theta) - TS\,(\theta,\ t - \Delta/2 \cos\theta)\right)$$

Results using this method were the same as those obtained using the previous method.

V. Numerical Results

Using the code developed from Section II and III, results were obtained for the radiation field response for a finite gap antenna. It was noted that the wave first reached the far field observation point when P1 > -1; in other words, when

$$\tau = -\sin\theta - \frac{\Delta}{2}\left|\cos\theta\right|, \tag{27}$$

This value of τ was called τ_β and a new variable for time, T, is defined as

$$T = \tau + \tau_\beta . \tag{28}$$

The variable a was always set to 1 since results were desired for Δ/a. Also, all of the results in this note are given for a radiation field normalized with respect to $\sin\theta$, i.e., $\sin \frac{rE_\theta}{V_o}$. Parameter studies are given in Figures 4 through 19 of this quantity with regard to T.

The radiation fields for various angles, θ for particular Δ/a's, are presented in Figures 4 through 9 with $\frac{2\theta}{\pi}$ as a parameter. It is noted that as the angle increases, the peak value increases, but the peak occurs earlier in time.

Figures 10 through 19 are graphs of the far field for a particular θ and with Δ/a as a parameter. Again, a generalization of the results can be made. As Δ/a increases, the peak occurs later in time, but the peak value decreases. It was noted that the peak occurred at

$$T = (\Delta/a)\cos\theta . \tag{29}$$

Using this as the peak time, calculations were done to create the graph in Figure 20. This graph illustrates the behavior of the peak for various Δ/a's with respect to θ.

It should also be noted that after the peak occurs, the behavior is similar to the behavior of an infinitesimal gap as described in Sensor and Simulation Note 73.

Comparison graphs of the early time asymptotic form and actual results are given in Figure 21. A summary curve of the time when the early time asymptotic form, given by equation (6), is within 1% of the actual result versus gap size is given in Figure 22.

The graphs of the late time asymptotic forms are given in Figure 23. It should be noted that agreement between the asymptotic form and the actual result is within the same accuracy range as those given for the infinitesimal gap.

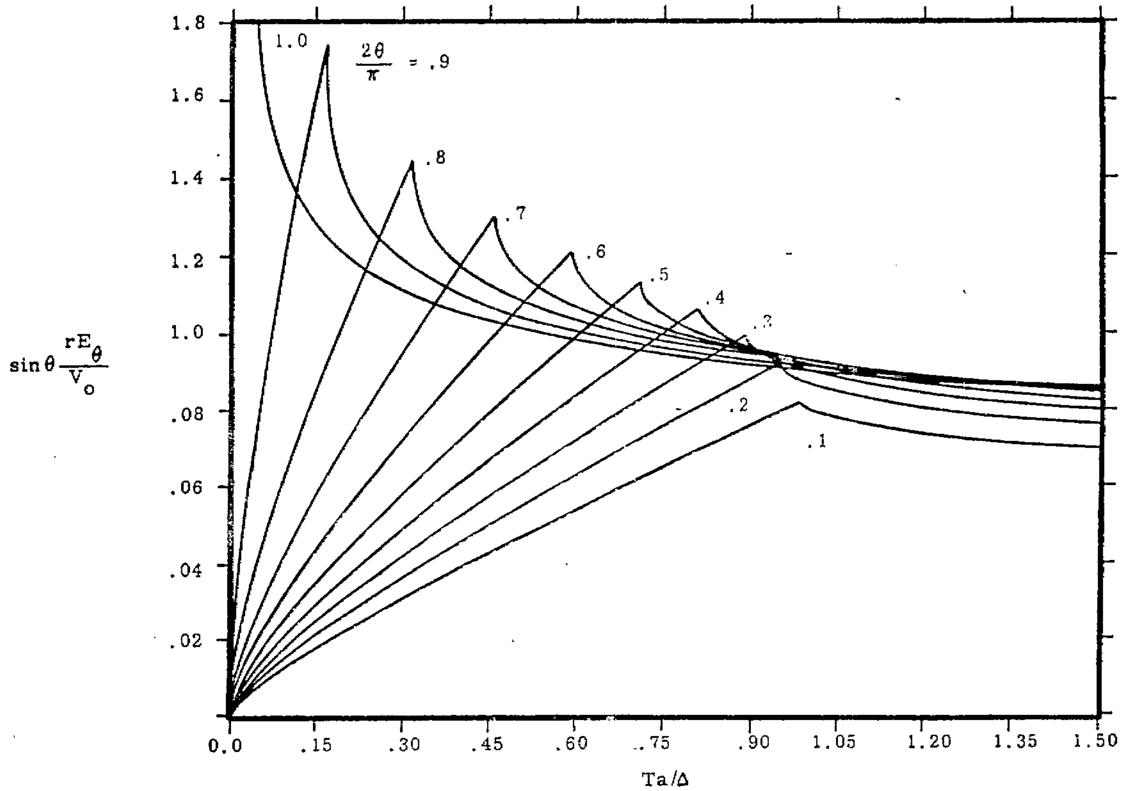

Figure 4. Radiation Field for $\Delta/a = 100$.

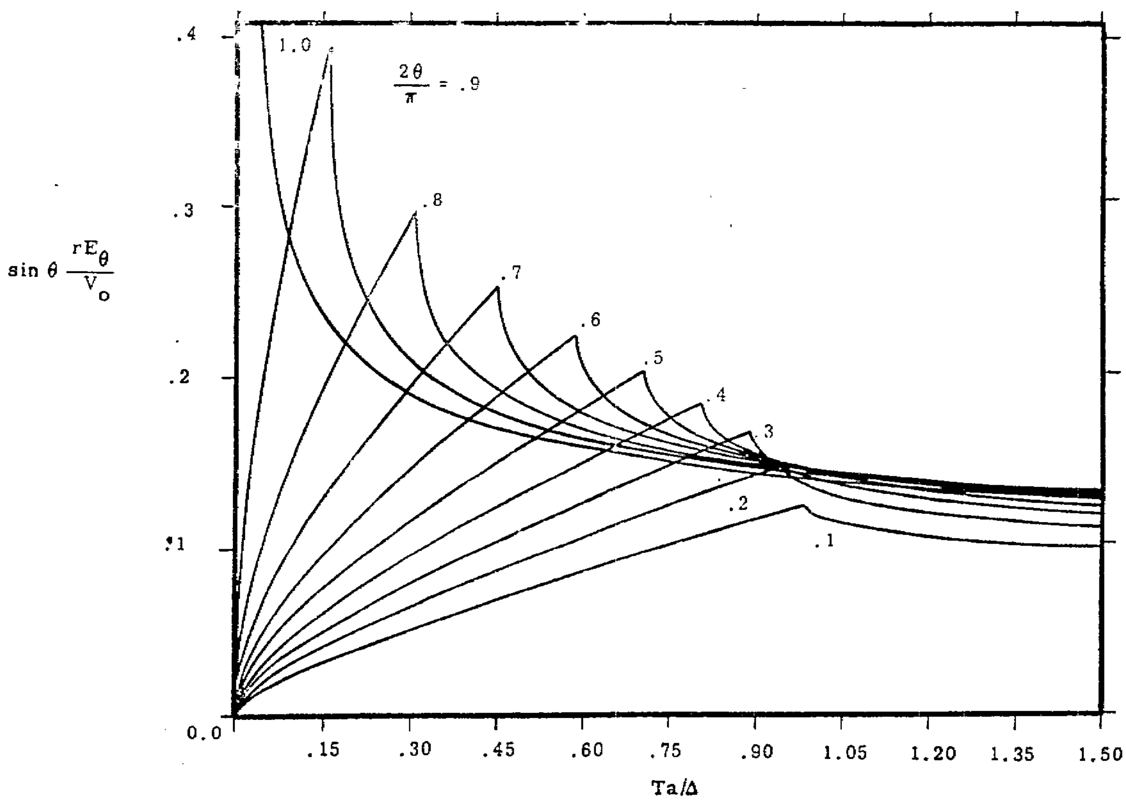

Figure 5. Radiation Field for $\Delta/a = 10$.

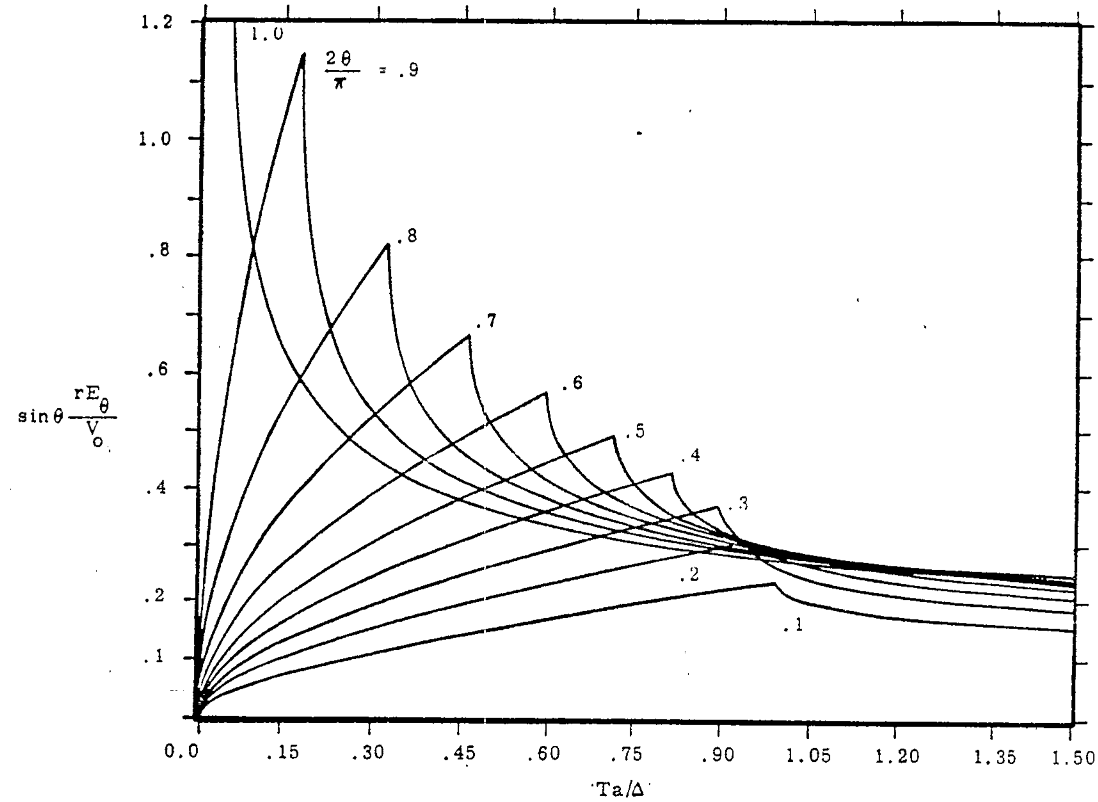

Figure 6. Radiation Field for Δ/a = 1.0

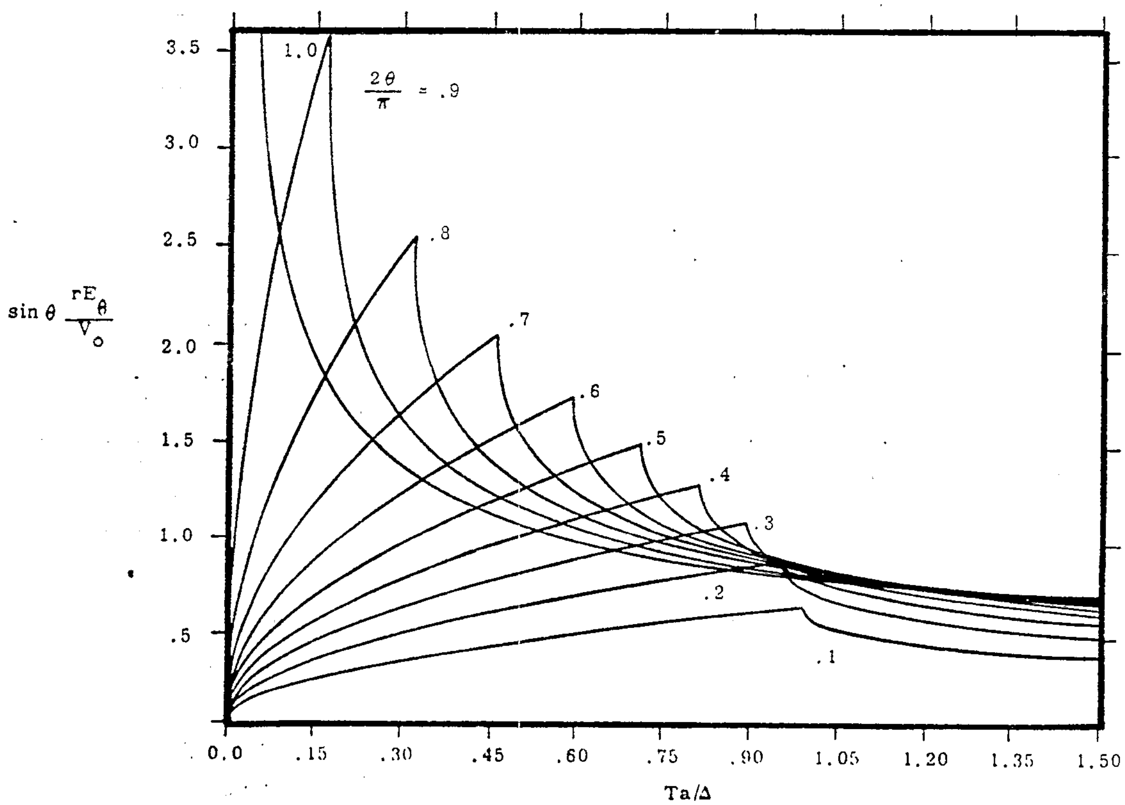

Figure 7. Radiation Field for Δ/a = .1

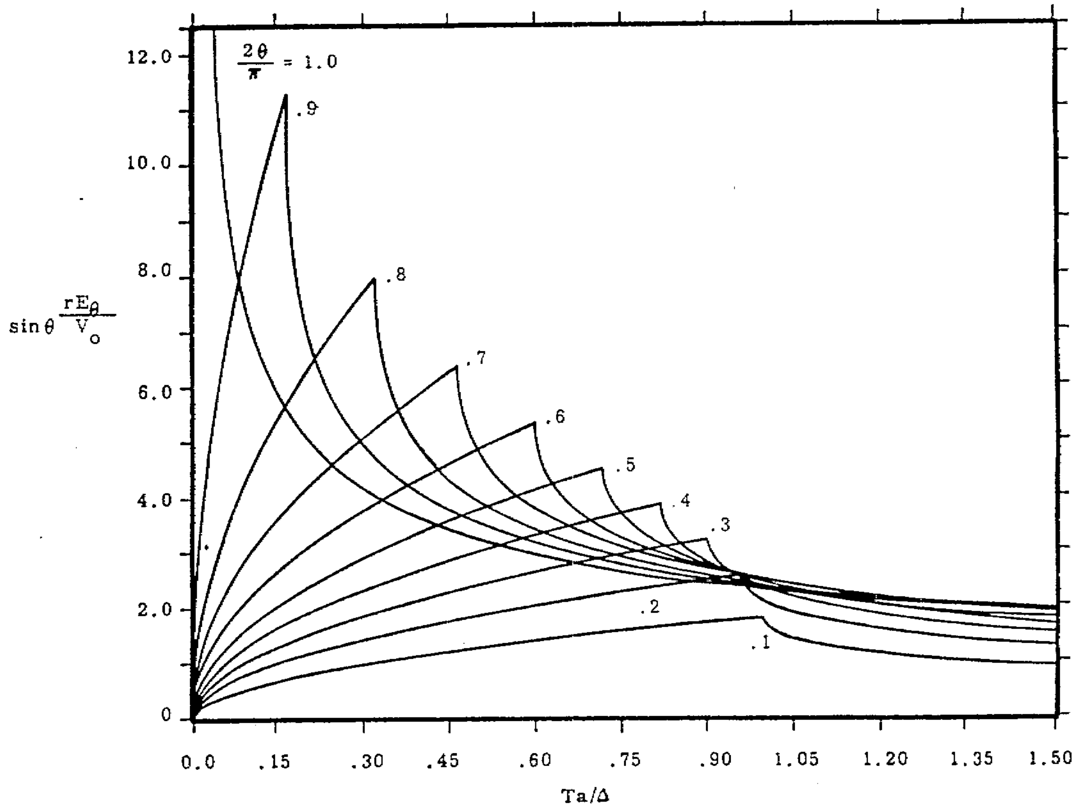

Figure 8. Radiation Field for Δ/a = .01

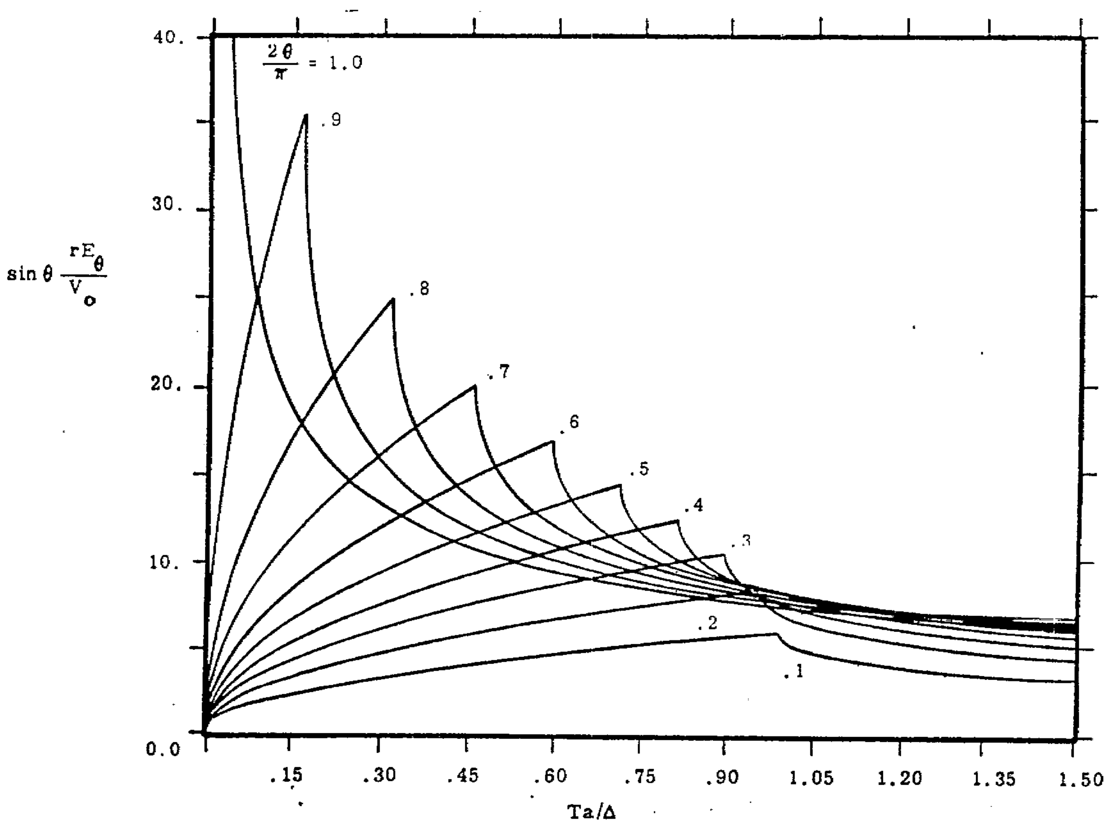

Figure 9. Radiation Field for Δ/a = .001

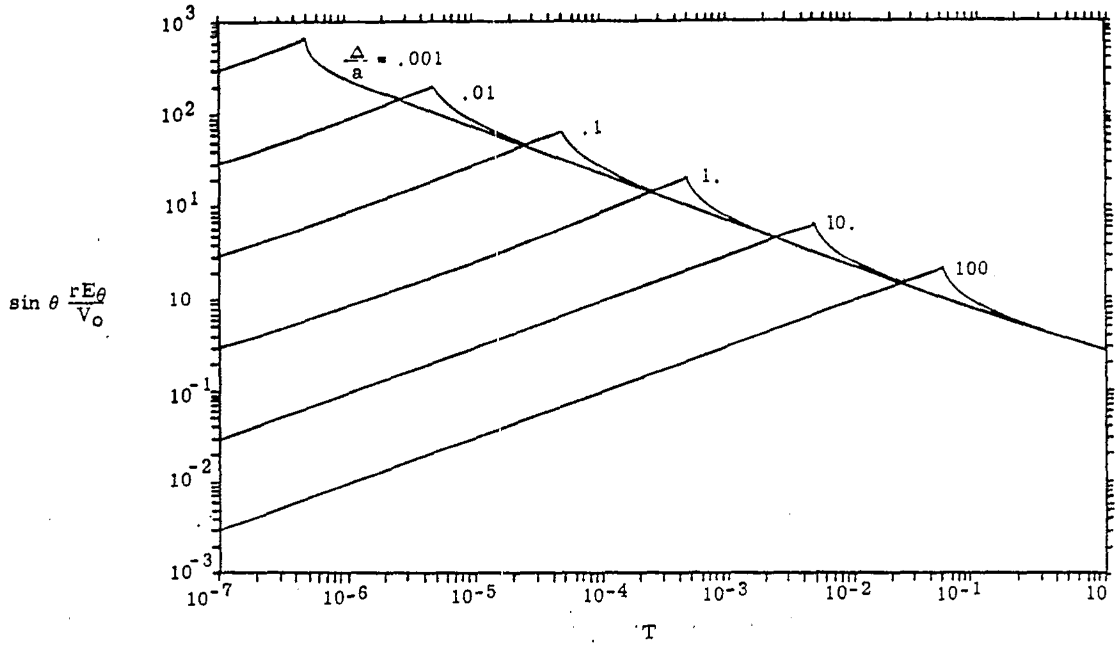

Figure 10. Radiation Field for $\frac{2\theta}{\pi}$ = .9995

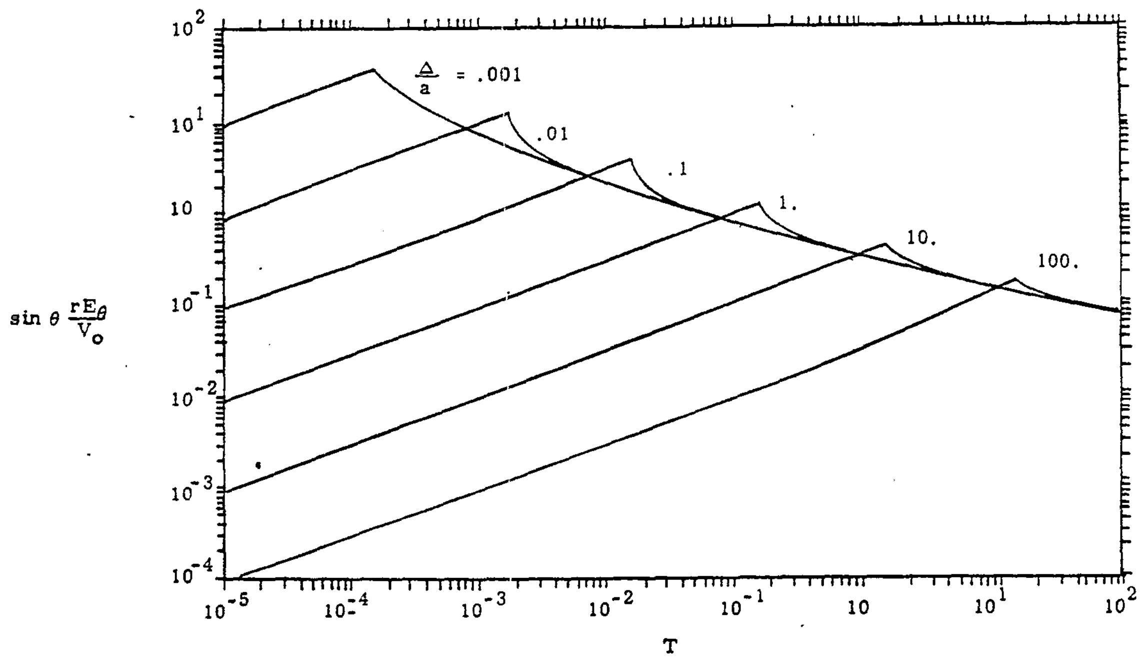

Figure 11. Radiation Field for $\frac{2\theta}{\pi}$ = .9

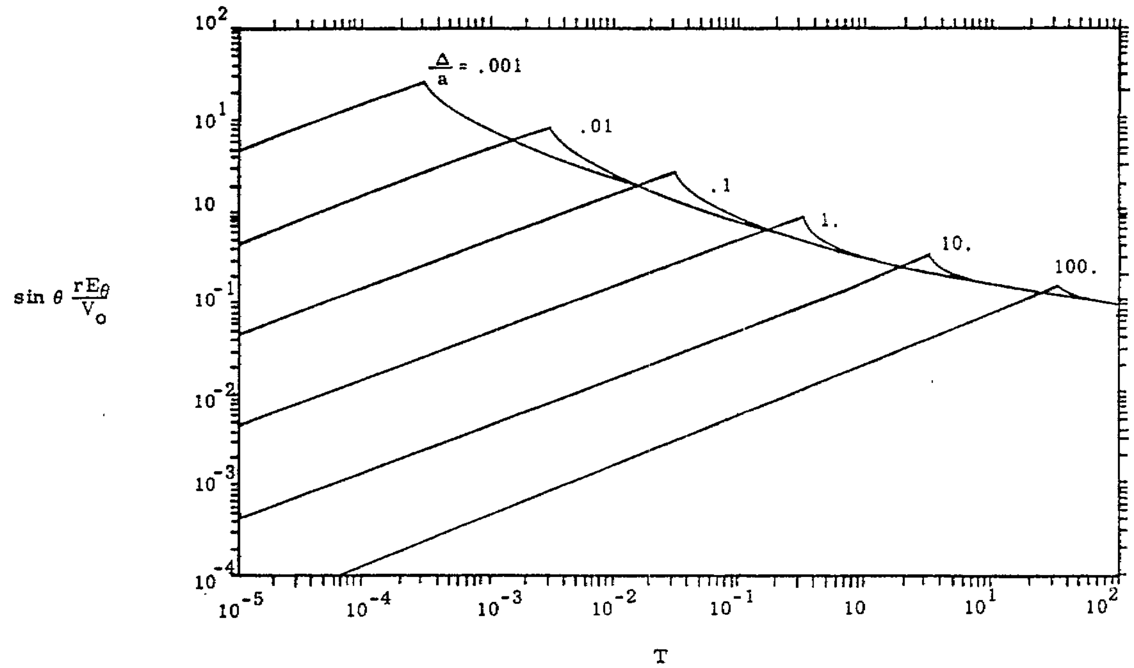

Figure 12. Radiation Field for $\frac{2\theta}{\pi} = .8$

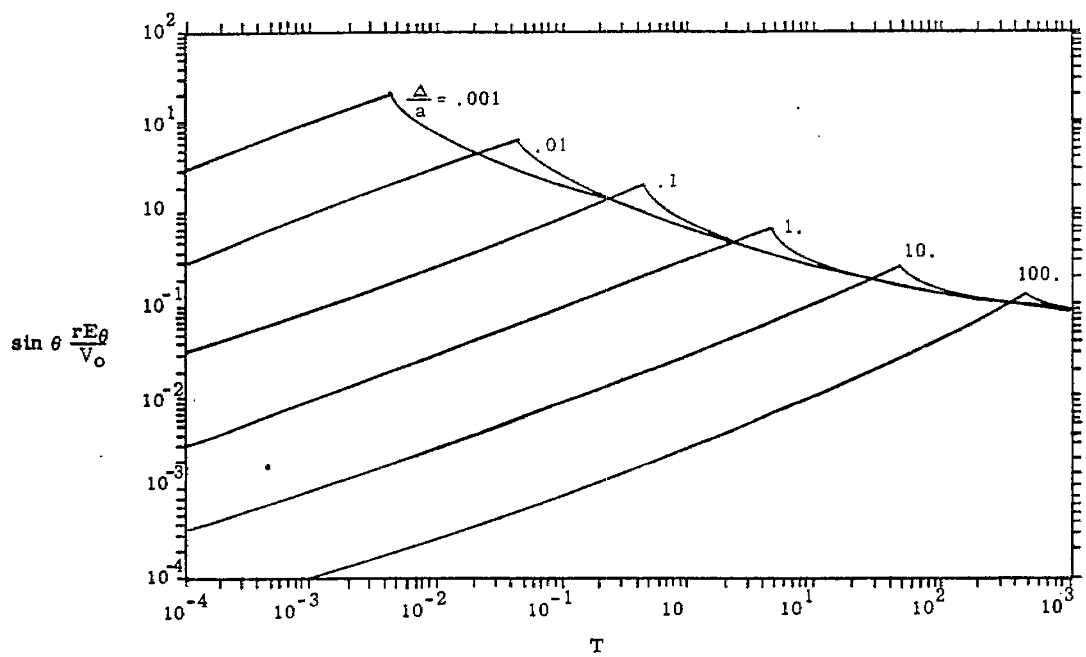

Figure 13. Radiation Field for $\frac{2\theta}{\pi} = .7$

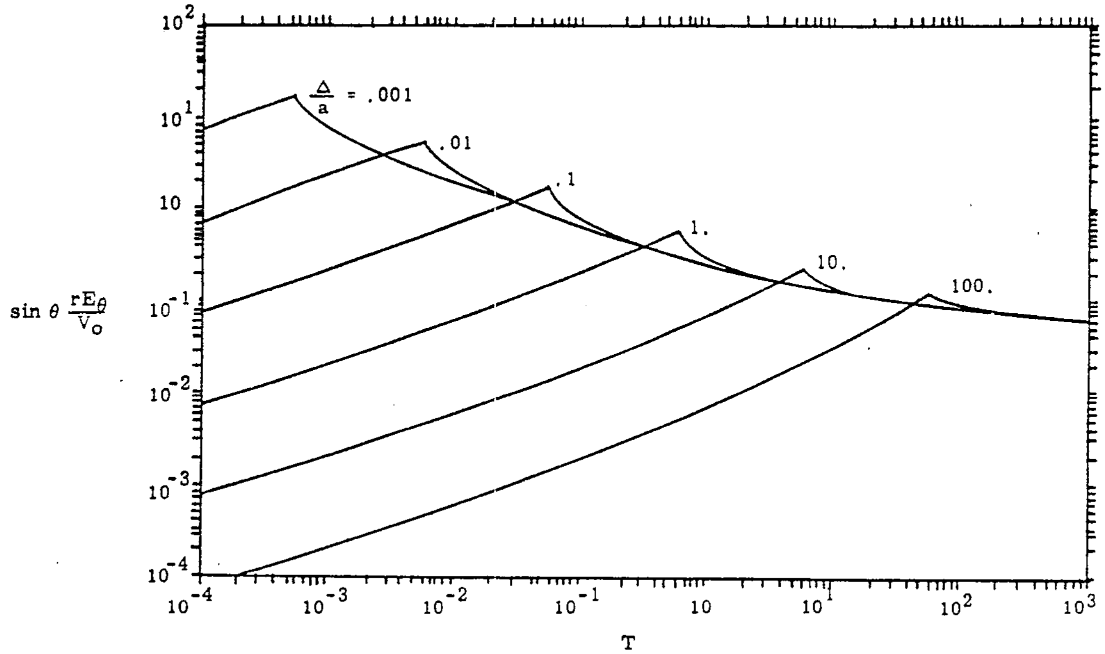

Figure 14. Radiation Field for $\frac{2\theta}{\pi}$ = .6

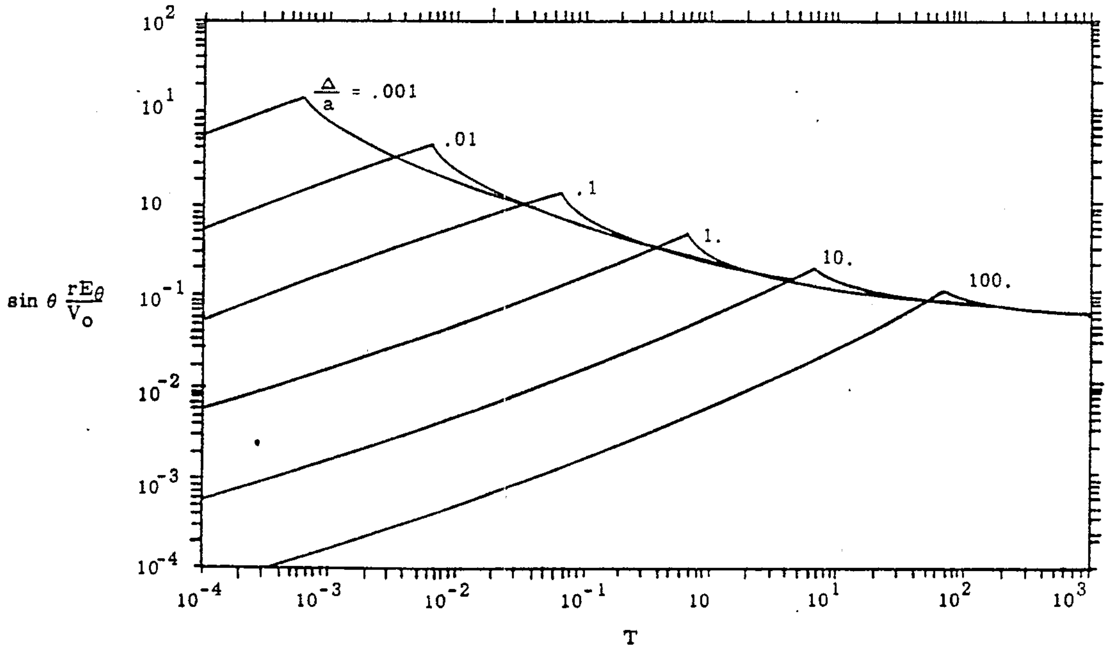

Figure 15. Radiation Field for $\frac{2\theta}{\pi}$ = .5

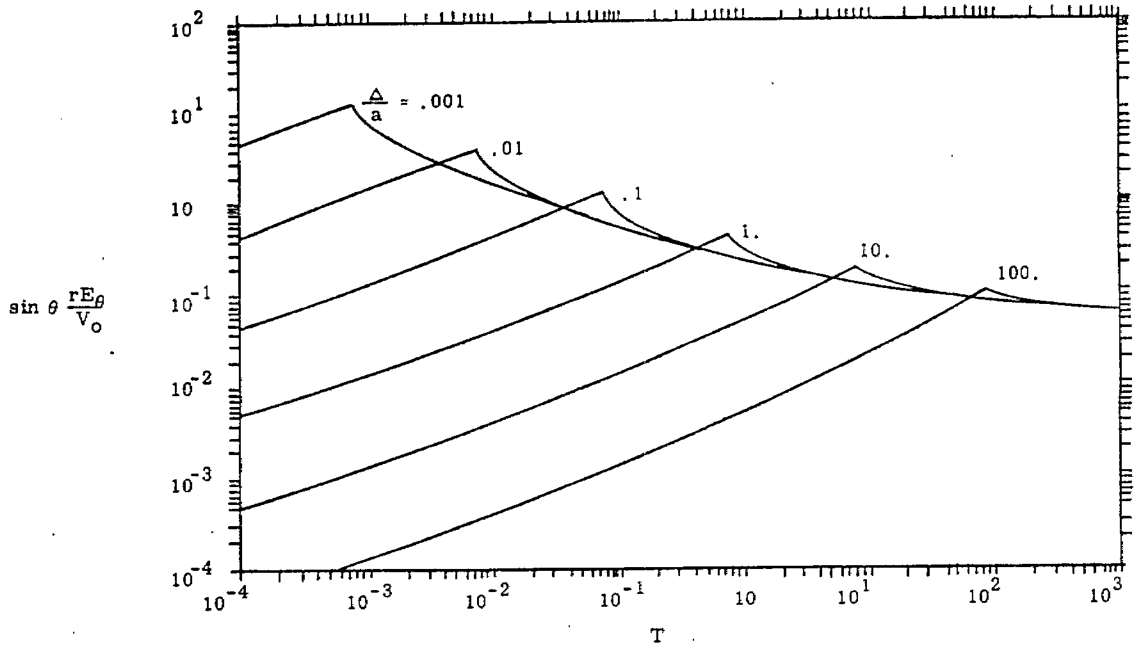

Figure 16. Radiation Field for $\frac{2\theta}{\pi} = .4$

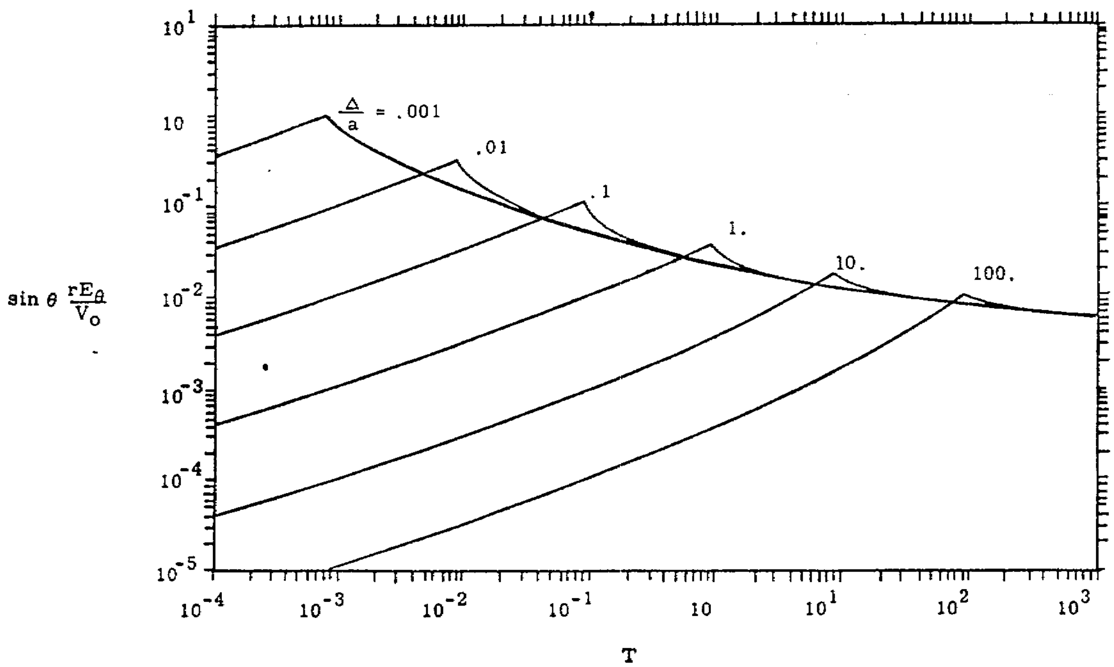

Figure 17. Radiation Field for $\frac{2\theta}{\pi} = .3$

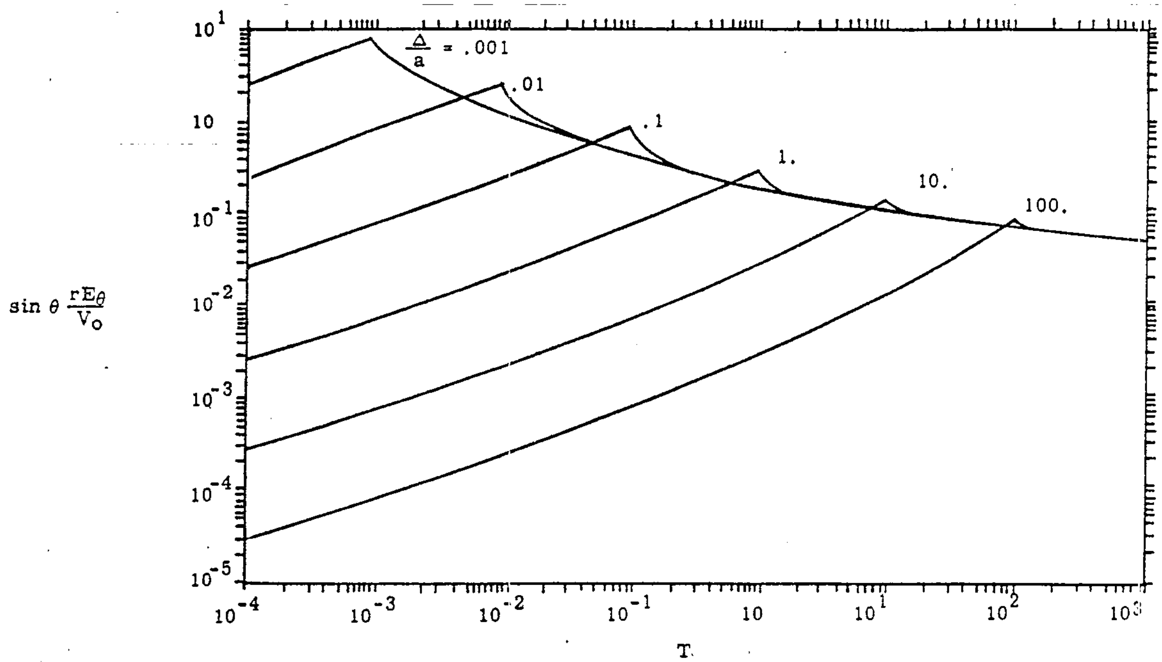

Figure 18. Radiation Field for $\frac{2\theta}{\pi}$ = .2

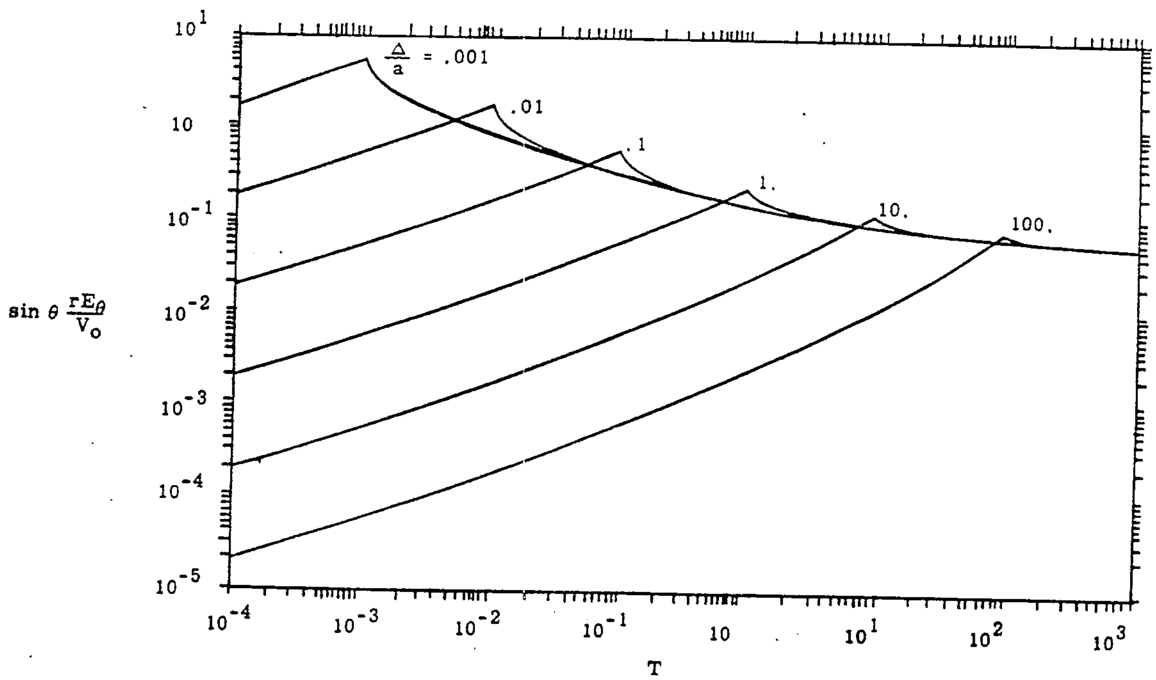

Figure 19. Radiation Field for $\frac{2\theta}{\pi}$ = .1

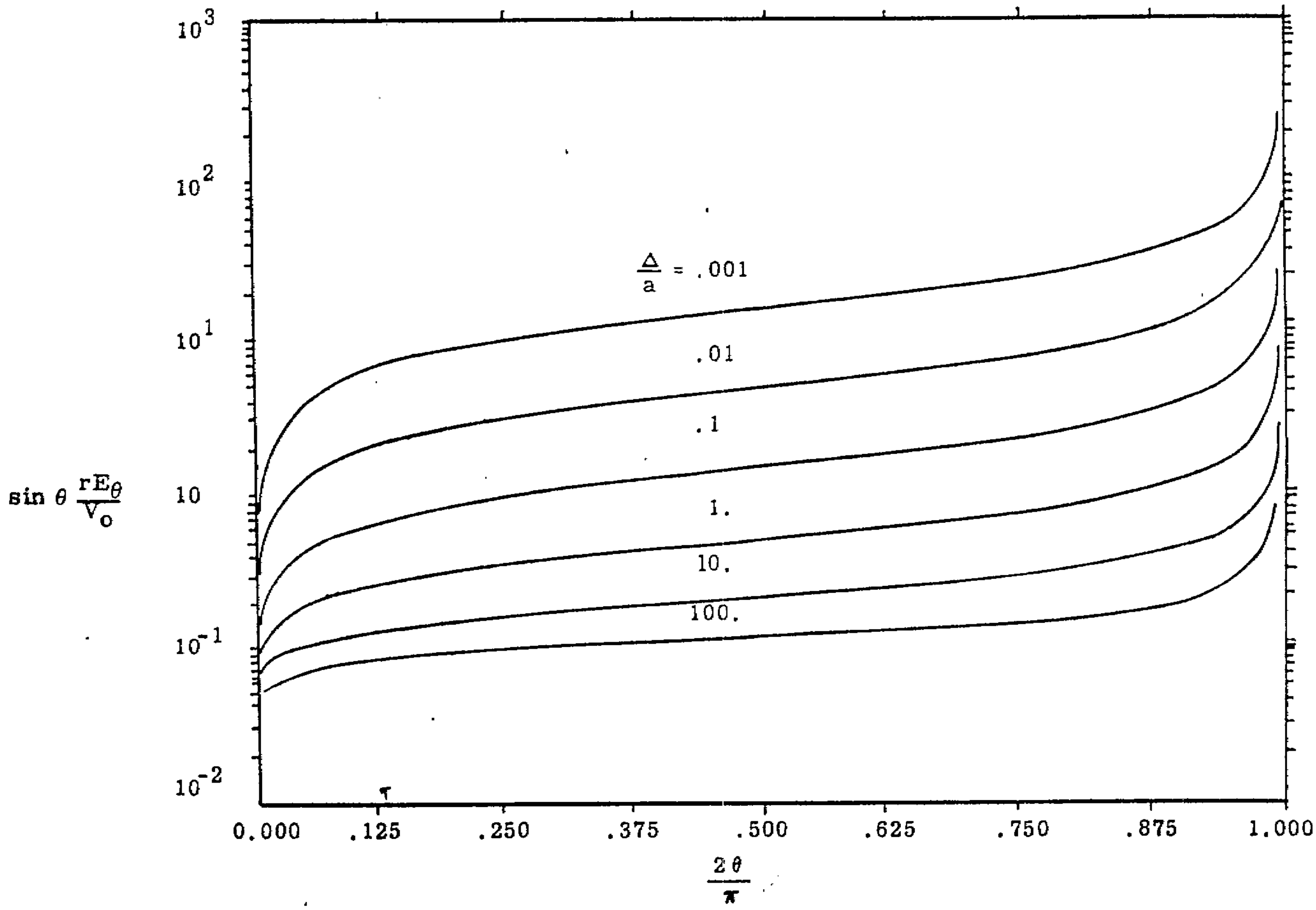

Figure 20. Peak Values of Radiation Field Versus Angle

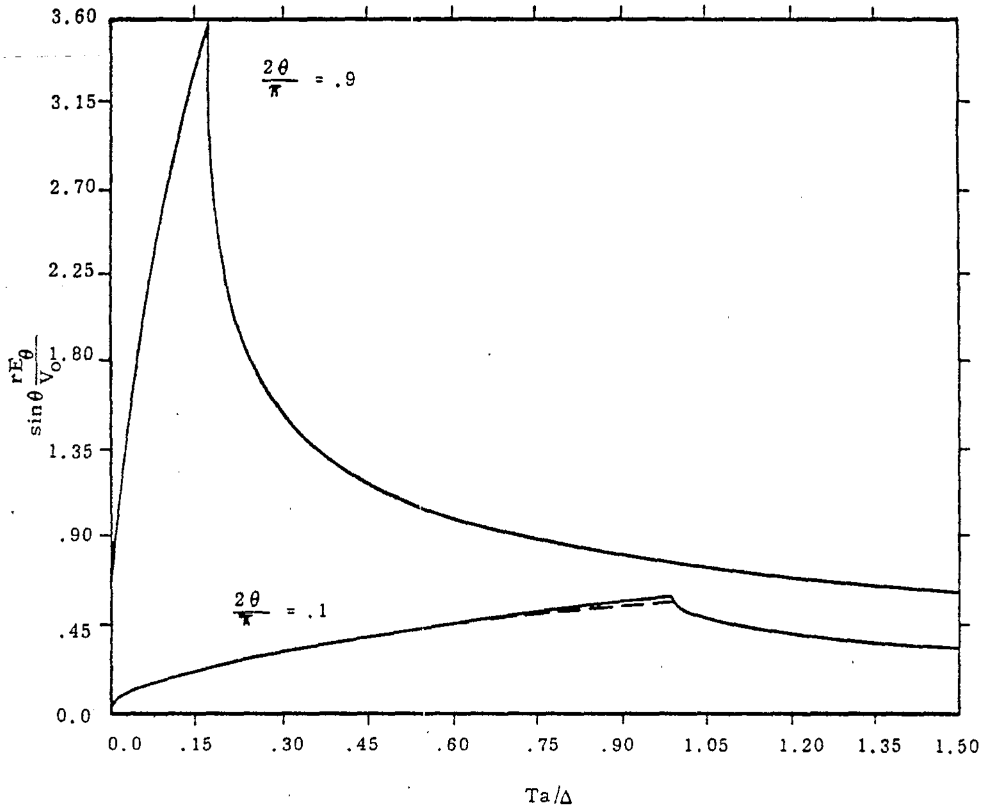

Figure 21a. Radiation Fields (solid) and asymptotic forms for early times (dotted) for $\Delta/a = .1$ and two values of θ.

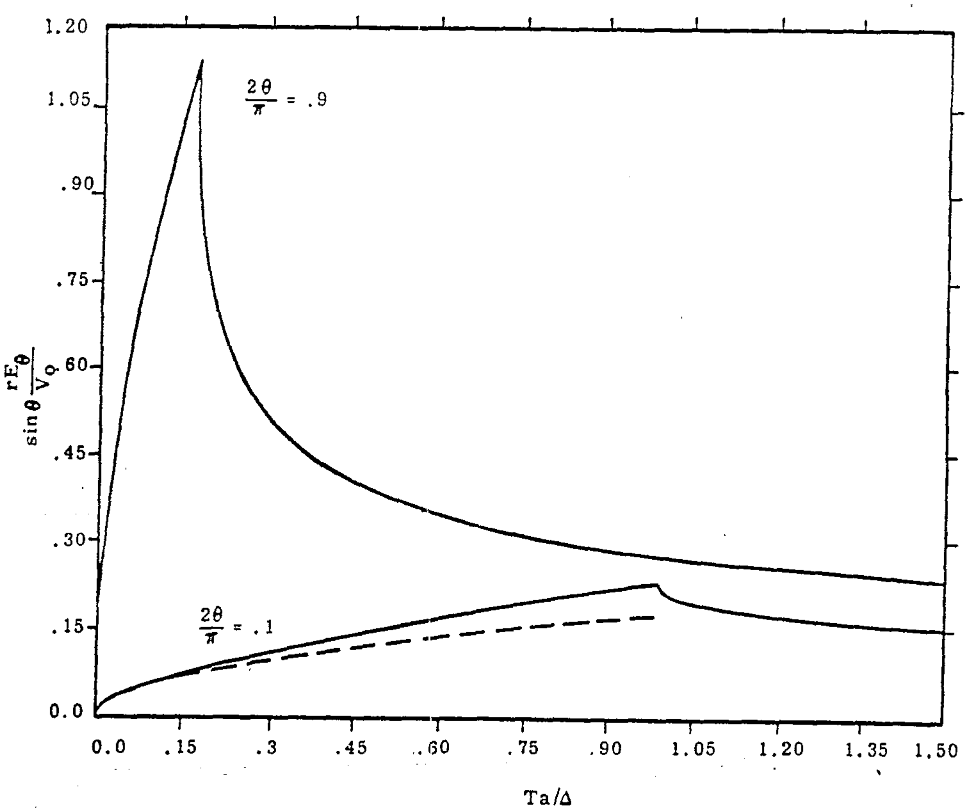

Figure 21b. Radiation Fields (solid) and asymptotic forms for early times (dotted) for $\Delta/a = 1.0$ and two values of θ.

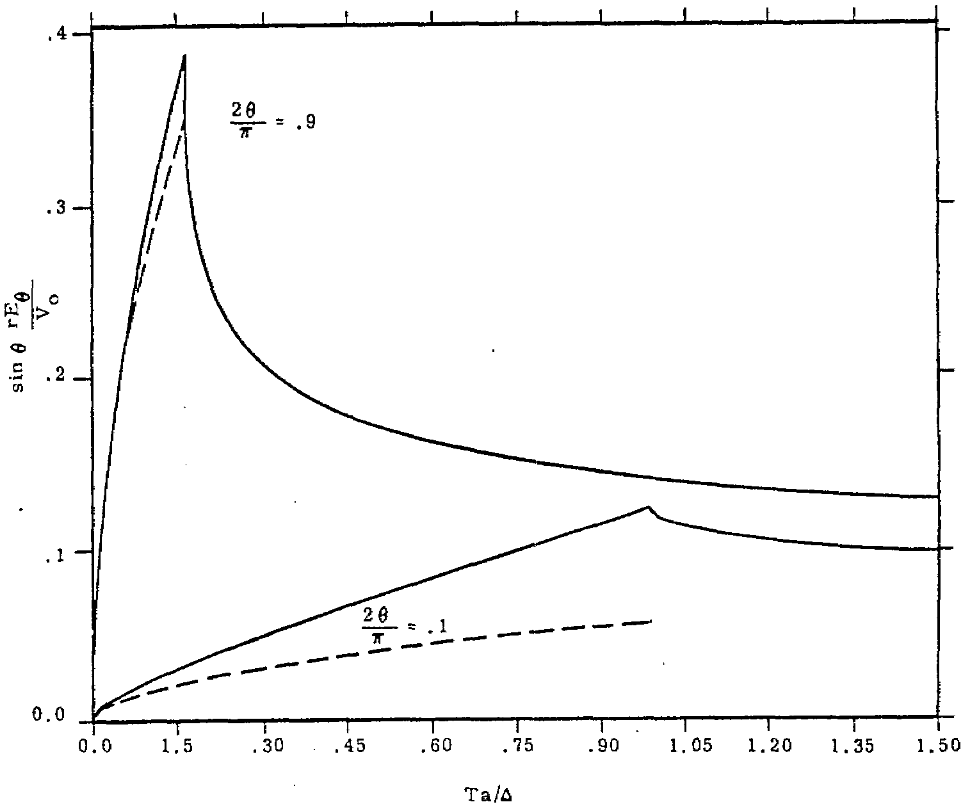

Figure 21c. Radiation Field (solid) and asymptotic form for early times (dotted) for $\Delta/a = 10$. and two values of θ.

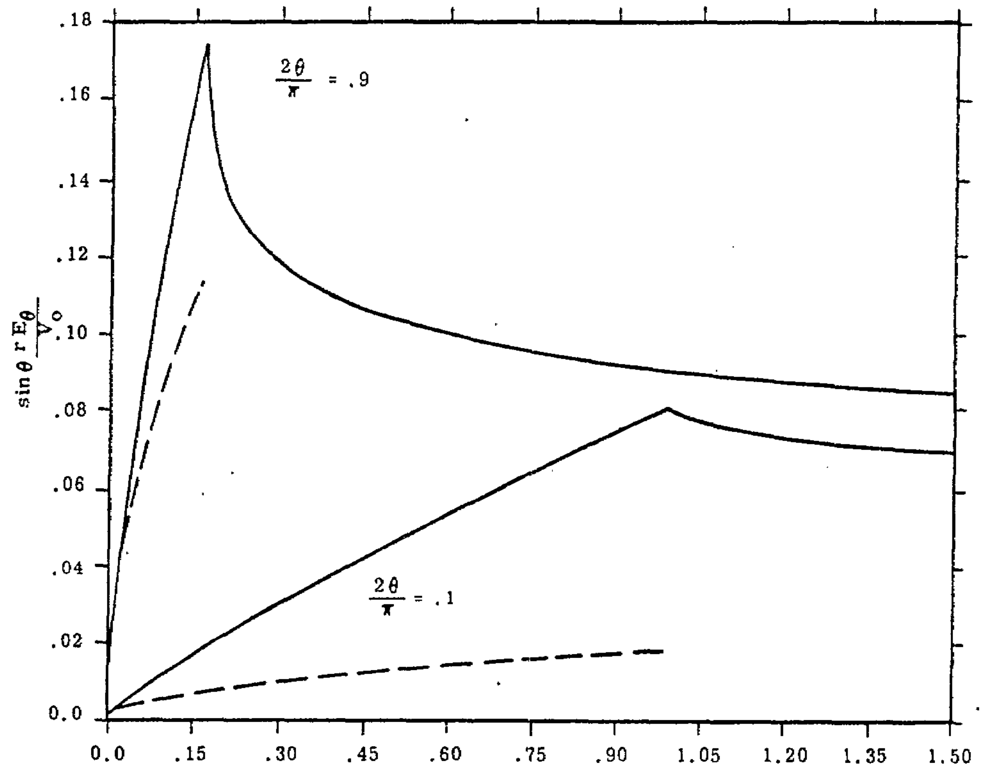

Figure 21d. Radiation Field (solid) and asymptotic form for early time (dotted) for $\Delta/a = 100$ and two values of θ.

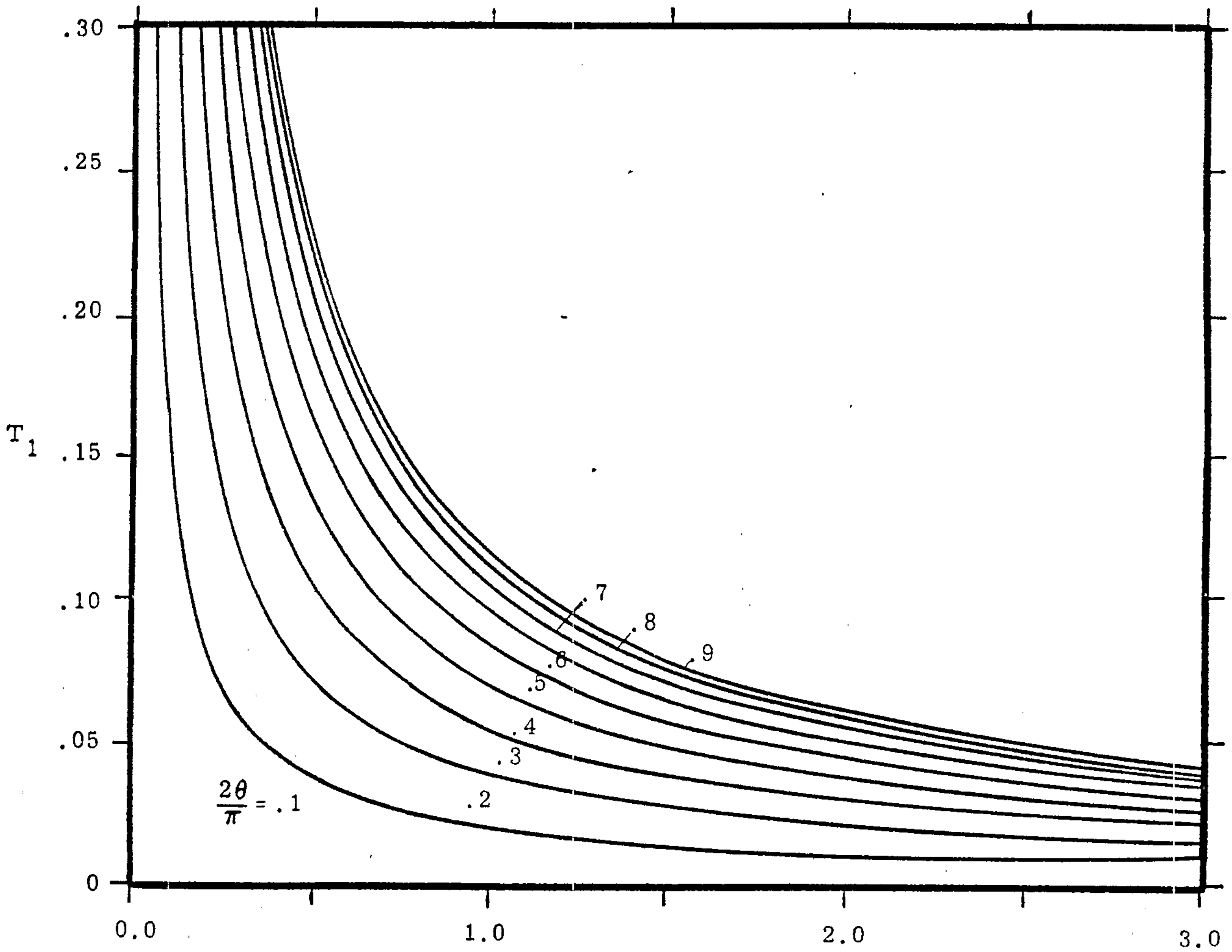

Figure 22. Plots of the time T_1 when the early time asymptotic value of the radiated field deviates from the actual value by 1%, as a function of Δ/a.

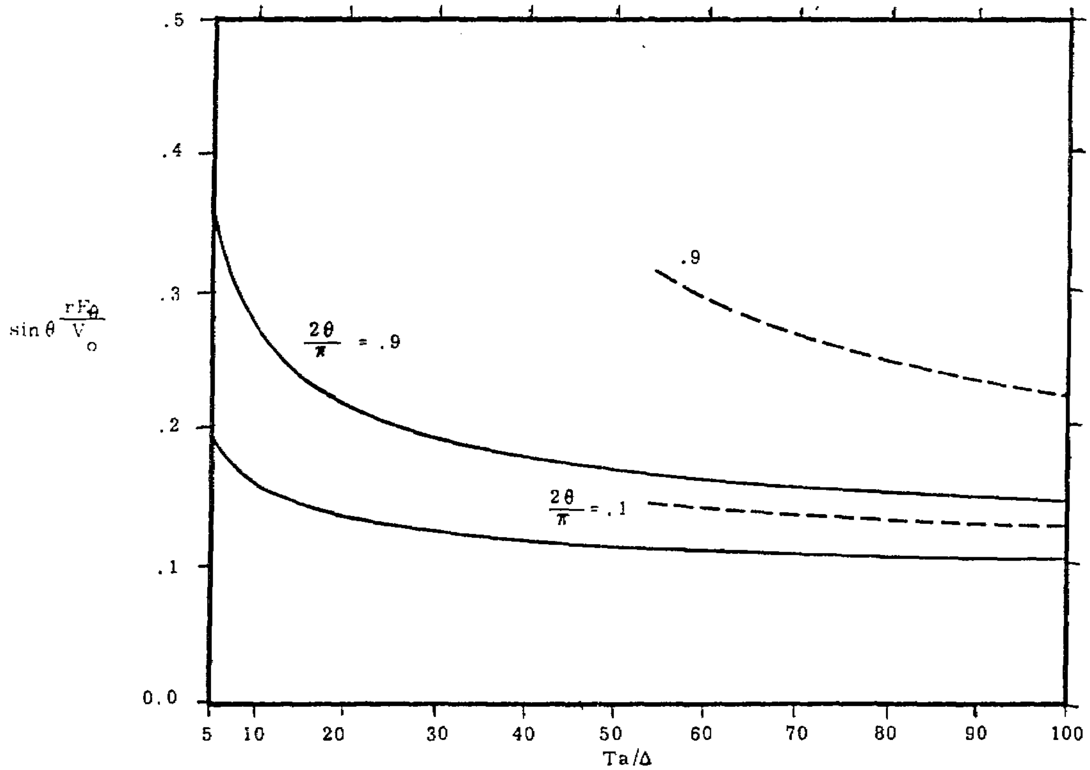

Figure 23a. Plots of the late time radiated field (solid) and the asymptotic field (dotted) for Δ/a = .1 and two values of θ.

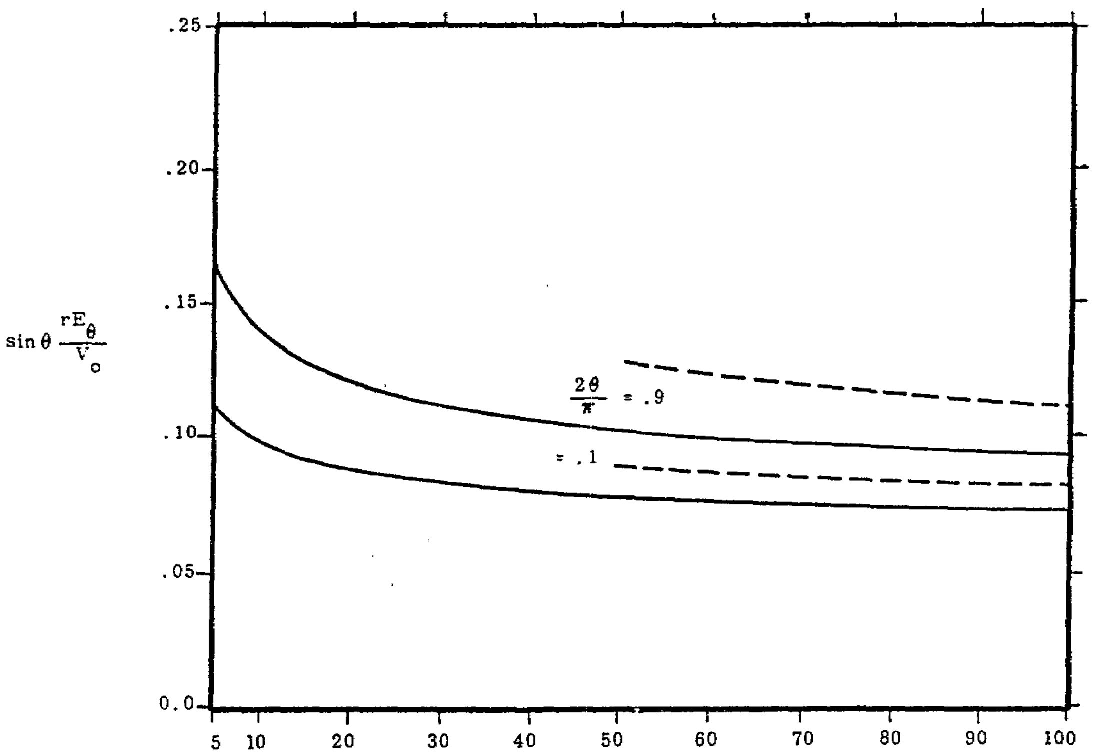

Figure 23b. Plots of the radiated field (solid) and the asymptotic field (dotted) for Δ/a = 1.0 and two values of θ.

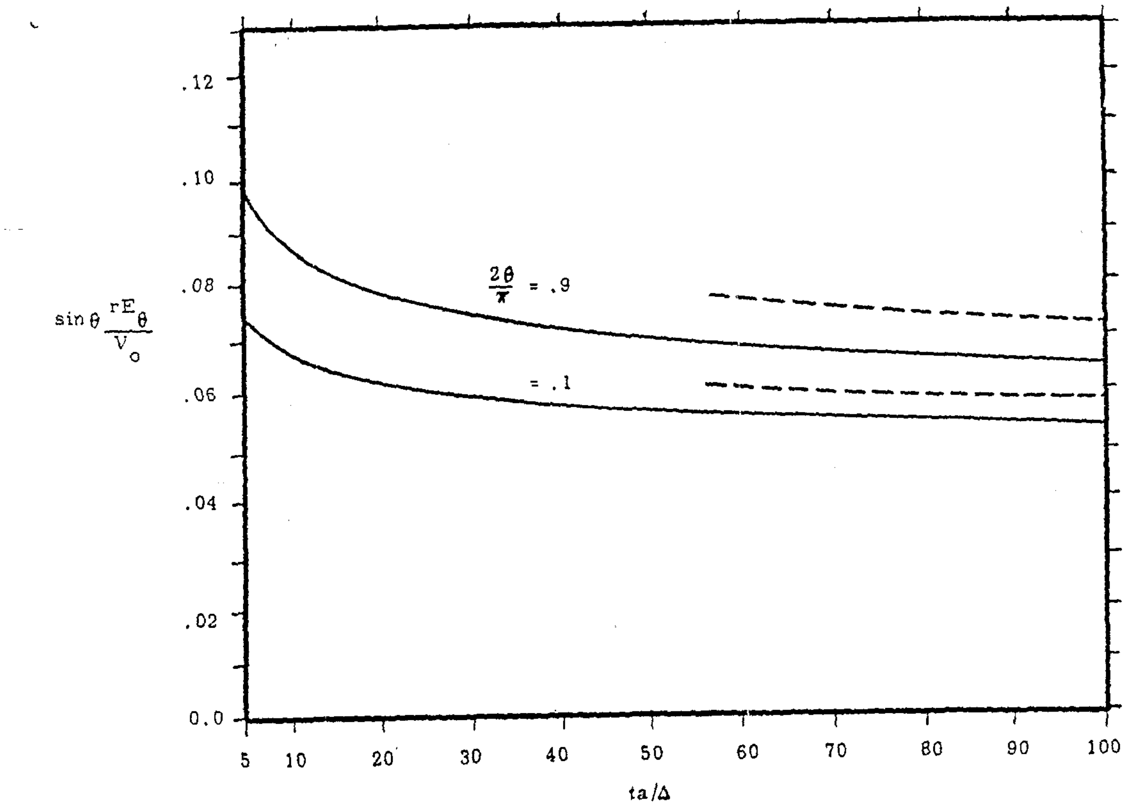

Figure 23c. Plots of the late time radiated field (solid) and the asymptotic field (dotted) for $\Delta/a = 10$ and two values of θ.

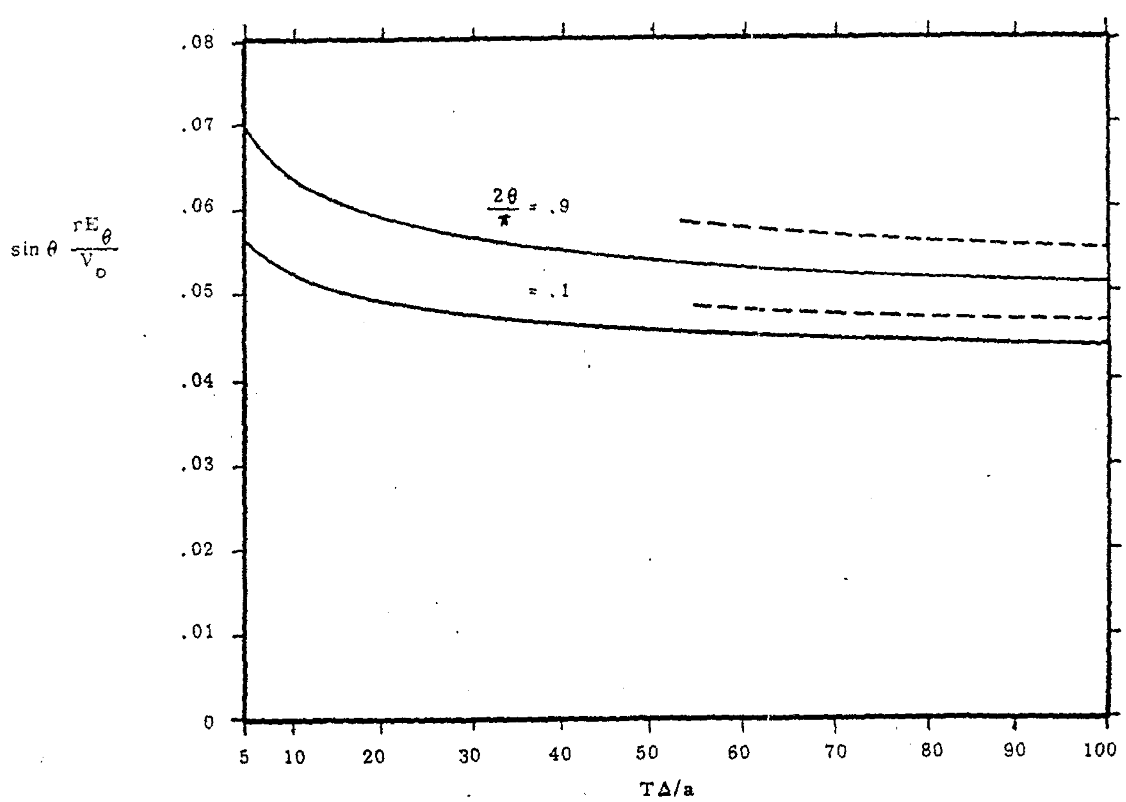

Figure 23d. Plots of the late time radiated field (solid) and the asymptotic field (dotted) for $\Delta/a = 100$ and two values of θ.

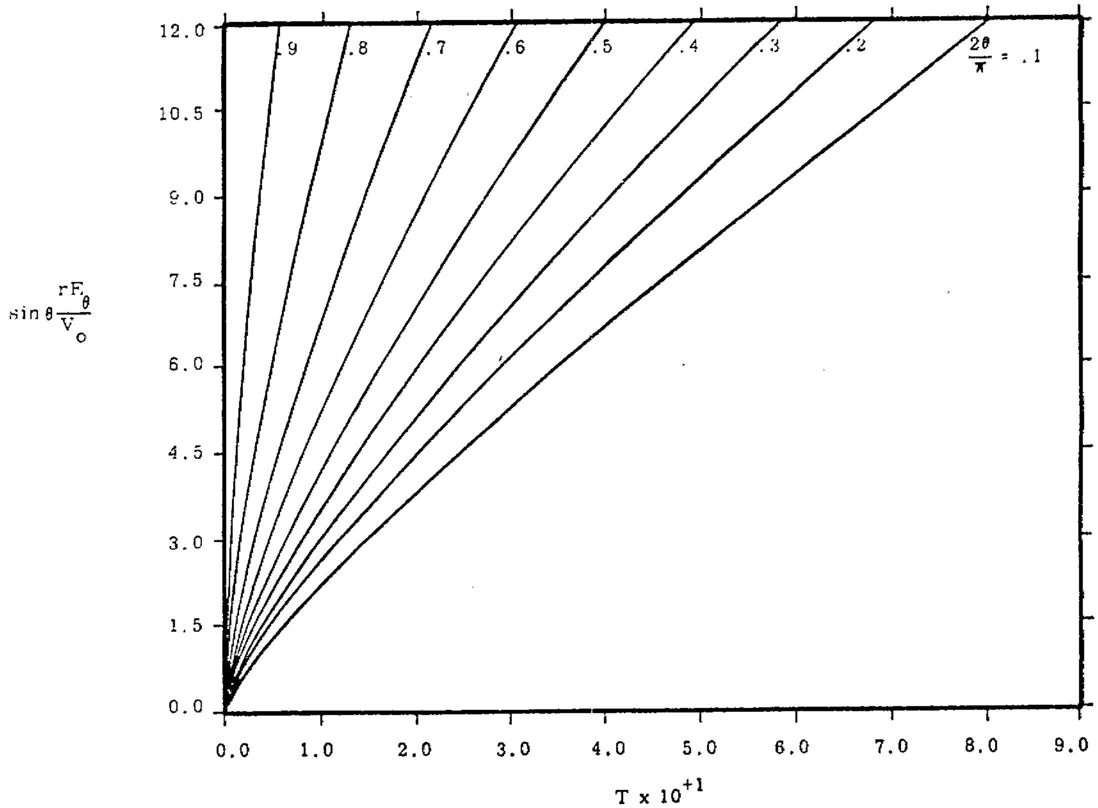

Figure 24. Radiation Field for the Semi-Infinite Gap

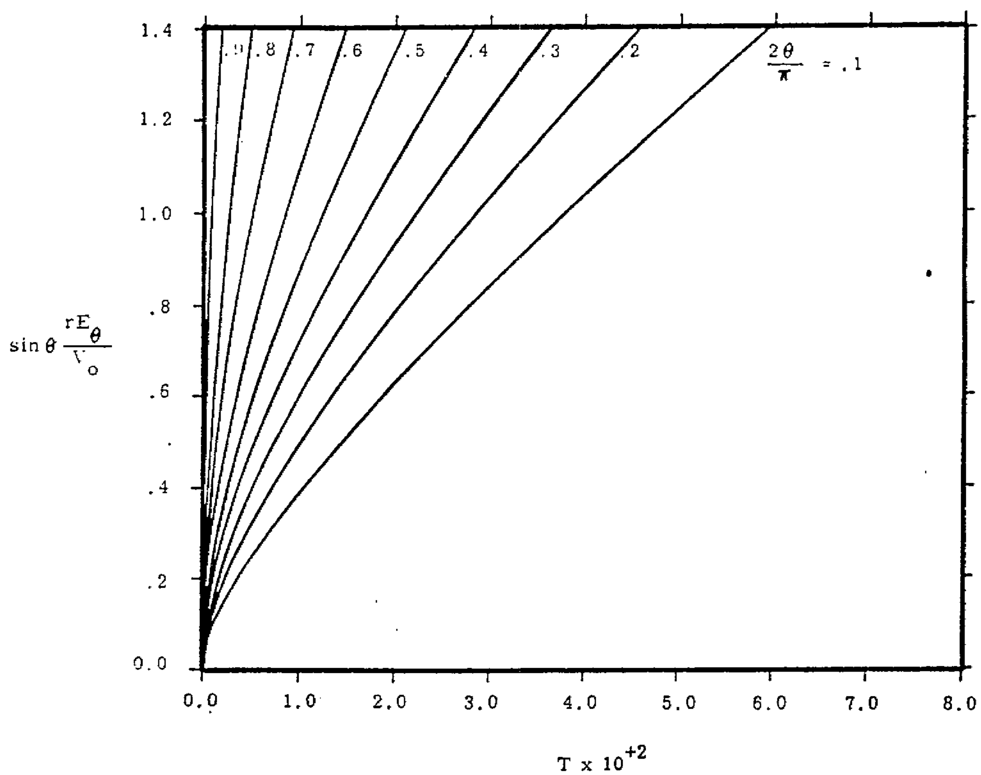

Figure 25. Radiation Field for the Semi-Infinite Gap

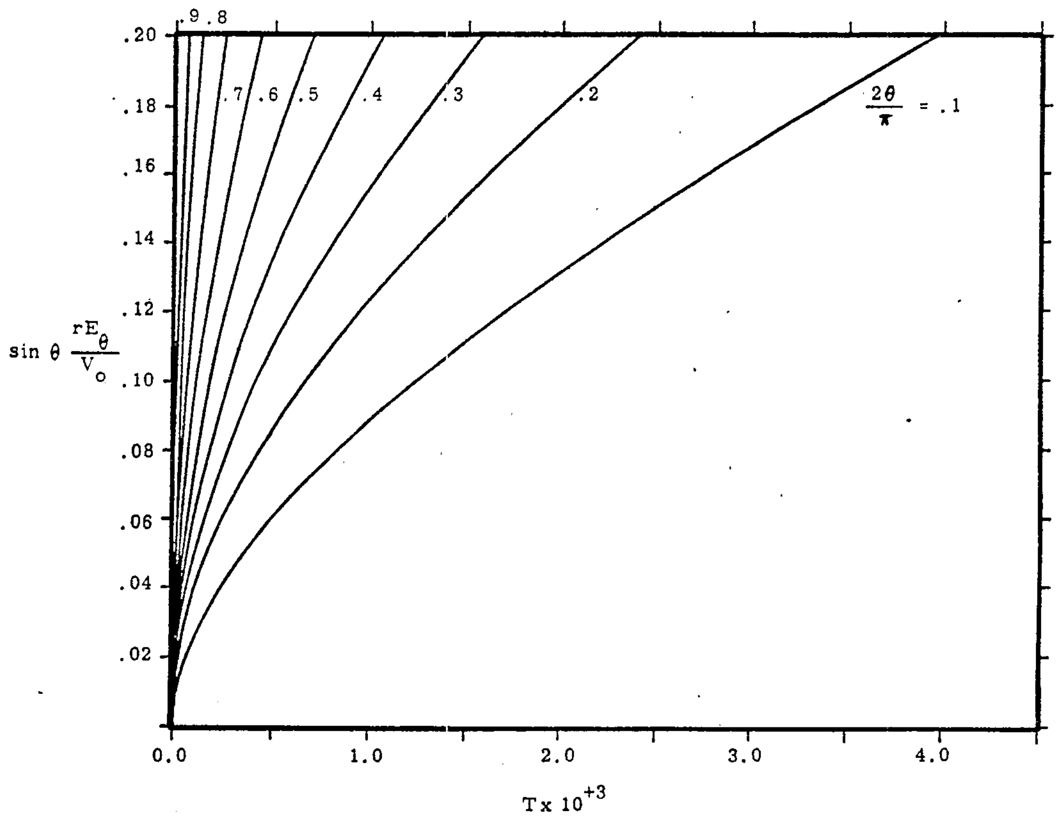

Figure 26. Radiation Field for the Semi-Infinite Gap (Early Time)

References

1. R. W. Latham, K. S. H. Lee, Sensor and Simulation Note 73, "Pulse Radiation and Synthesis by an Infinite Cylindrical Antenna," February, 1969.

2. Paul R. Barnes, Sensor and Simulation Note 110, "Pulse Radiation by an Infinitely Long, Perfectly Conducting, Cylindrical Antenna in Free Space Excited by a Finite Cylindrical Distributed Source Specified by the Tangential Electric Field Associated with a Biconical Antenna," July, 1970.